ChemMedChem

Research Article
doi.org/10.1002/cmdc.202300506

Chemistry Europe
European Chemical Societies Publishing

www.chemmedchem.org

Carboranes as Potent Phenyl Mimetics: A Comparative Study on the Reversal of ABCG2-Mediated Drug Resistance by Carboranylquinazolines and Their Organic Isosteres

Philipp Stockmann[+],[a] Lydia Kuhnert[+],*[b] Tamara Krajnović,[c] Sanja Mijatović,[c] Danijela Maksimović-Ivanić,[c] Walther Honscha,[b] and Evamarie Hey-Hawkins*[a]

Multidrug resistance is a major challenge in clinical cancer therapy. In particular, overexpression of certain ATP-binding cassette (ABC) transporter proteins, like the efflux transporter ABCG2, also known as breast cancer resistance protein (BCRP), has been associated with the development of resistance to applied chemotherapeutic agents in cancer therapies, and therefore targeted inhibition of BCRP-mediated transport might lead to reversal of this (multidrug) resistance (MDR). In a previous study, we have described the introduction of a boron-carbon cluster, namely *closo*-dicarbadodecaborane or carborane, as an inorganic pharmacophore into a polymethoxylated 2-phenylquinazolin-4-amine backbone. In this work, the scope was extended to the corresponding amide derivatives. As most of the amide derivatives suffered from poor solubility, only the amide derivative **QCe** and the two amine derivatives **DMQCc** and **DMQCd** were further investigated. Carboranes are often considered as sterically demanding phenyl mimetics or isosteres. Therefore, the organic phenyl and sterically demanding adamantyl analogues of the most promising carborane derivatives were also investigated. The studies showed that the previously described **DMQCd**, a penta-methoxylated *N*-carboranyl-2-phenylquinazolin-4-amine, was by far superior to its organic analogues in terms of cytotoxicity, inhibition of the human ABCG2 transporter, as well as the ability to reverse BCRP-mediated mitoxantrone resistance in MDCKII-hABCG2 and HT29 colon cancer cells. Our results indicate that **DMQCd** is a promising candidate for further in vitro as well as in vivo studies in combination therapy for ABCG2-overexpressing cancers.

Introduction

Barely any other field has gained as much momentum in recent years on the clinical pharmacokinetics of drugs as the various transmembrane-uptake and -efflux transporters found in different tissues of the human body. A vast spectrum of molecules, like nutrients, cytostatic drugs or small molecule inhibitors, are high-affinity substrates of these transporters and are transported into or from the cell via these carriers.[1] A majority of efflux transporters belong to the superfamily of ATP-binding cassette (ABC) transporter proteins.[2] By generating energy through ATP hydrolysis, substrates are transported out of the cell against a concentration gradient. Among seven subfamilies of ABC proteins – A to G – the 48 members are categorized based on their amino acid sequences, domain array, phylogenetics, or gene structure.[3] Specifically, the breast cancer resistance protein (BCRP, ABCG2) is expressed in several tissue barriers such as placenta, blood-testis or blood-brain barrier, and mediates the efflux of a broad array of compounds.[4] Further, as a multidrug transporter it is responsible for the outward transfer of several antineoplastic and anti-tumor agents, and thus, associated with multidrug resistance (MDR) in cancer.[5,6] Over the past years, a number of studies have been published, providing extended understanding of the BCRP concerning physiological functionality, substrate spectrum, locations and polymorphism.[7,8] Nevertheless, no inhibitor or modulator is yet in use for addressing BCRP as a therapeutic target in clinical applications, although its role in MDR and substrate-specificity toward relevant anti-neoplastic agents like tyrosine kinase inhibitors, mitoxantrone or camptothecins are known (Figure 1A–C).[6,7,9] Thus, further exploration of novel BCRP-addressing inhibitors with high potency to inhibit the human ABCG2 transporter and reverse multidrug resistance in ABCG2-overexpressing cell lines, while possessing non-toxic properties, is needed.

Recently, we presented the successful implementation of a hybrid inorganic-organic framework – *closo*-dicarbadodecaborane or carborane ($C_2B_{10}H_{12}$), consisting of an icosahedral boron-

[a] *Dr. P. Stockmann,[+] Prof. E. Hey-Hawkins*
Faculty of Chemistry and Mineralogy
Leipzig University
Johannisallee 29, 04103 Leipzig (Germany)
E-mail: hey@uni-leipzig.de

[b] *Dr. L. Kuhnert,[+] Prof. W. Honscha*
Faculty of Veterinary Medicine
Leipzig University
An den Tierkliniken 15, 04103 Leipzig (Germany)
E-mail: lydia.kuhnert@vetmed.uni-leipzig.de

[c] *Dr. T. Krajnović, Prof. S. Mijatović, Prof. D. Maksimović-Ivanić*
Institute for Biological Research "Sinisa Stankovic"
University of Belgrade
Bul. despota Stefana 142, 11108 Belgrade (Serbia)

[+] *These authors contributed equally to this work.*

Supporting information for this article is available on the WWW under https://doi.org/10.1002/cmdc.202300506

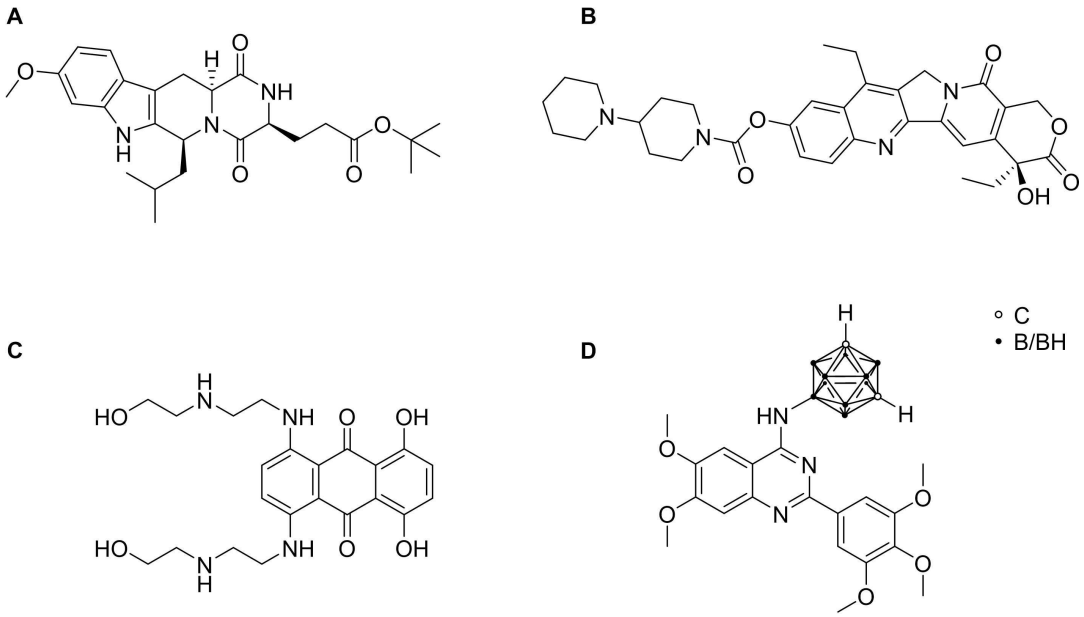

Figure 1. (**A**) Molecular structure of the reference compound Ko143; (**B**) camptothecin derivative and topoisomerase inhibitor irinotecan; (**C**) antineoplastic agent mitoxantrone (MXN); (**D**) carboranyl quinazoline-based BCRP inhibitor **DMQCd**.

carbon cluster – as pharmacophore into a polymethoxylated 2-phenylquinazolin-4-amine structure (**DMQCd**, Figure 1D), resulting in a strong inhibitor of the human ABCG2 protein and a strong reverser of BCRP.[10] Carboranes have gained increasing attention in recent years as their special properties make them particularly interesting for medicinal applications.[11] Furthermore, carborane-based derivatives were investigated for targeting other pathways in tumor progression and as boron-rich reagents for use in boron neutron capture therapy (BNCT).[10,12] The high hydrophobicity of this moiety may enhance the permeability of the drug through lipophilic cell membranes or increase substrate-protein interactions to cause more potent inhibition or modulation of the protein. The application of carboranes in pharmacological compounds was often approached by its similarity to a three-dimensional phenyl ring, with carboranes being used as phenyl mimetics. However, studies often lack direct comparison to organic analogues, the efficacy of the carborane compound is lower than that of the phenyl analogue, or the often-promised improved metabolic stability due to its inorganic nature remains unanswered.[13]

Our previous studies led to the discovery of potent ABCG2 inhibitors and reversers of ABCG2-mediated MDR.[14] In this work, we report the synthesis of *N*-carboranoyl-2-phenylquinazolin-4-amines, an extension of quinazoline amines to quinazoline amides maintaining the parent (poly-)methoxylated quinazolin-4-amine structure (Figure 2). The new compounds were evaluated for their cytotoxicity and ability to inhibit BCRP. Furthermore, phenyl and adamantyl analogues of the most efficient carboranyl derivatives were prepared and evaluated for their toxicity and inhibitory activity against human ABCG2. In a final step, the ability of the novel compounds to reverse the ABCG2-mediated mitoxantrone resistance was investigated in MDCKII-hABCG2 and HT29 colon cancer cells.

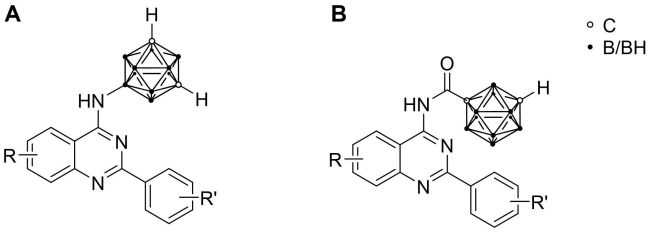

Figure 2. General structure of (un-)substituted (**A**) *N*-(*meta*-carboran-9-yl)-2-phenylquinazolin-4-amines[14] and (**B**) *N*-(*meta*-carboran-1-oyl)-2-phenylquinazolin-4-amines.

Results and Discussion

Syntheses

Synthesis of substituted 2-phenylquinazolin-4-amine derivatives can be accomplished by different synthetic strategies. As described in our previous work,[14] quinazolin-4-amines **Qa**–**d** and **DMQa**–**d** were prepared following a procedure by van Muijlwijk-Koezen et al..[15] In order to expand the variety of potential inhibitors, the carboranyl amides **QCe**–**h** and **DMQCe**–**g** were prepared by reacting amines **Qa**–**d** and **DMQa**–**d** with *closo*-1,7-dicarbadodecaborane-1-carbonyl chloride (**CbCOCl**,[16] Scheme 1c). Unfortunately, the penta-methoxylated amide derivative (**DMQCh**) as an analogue of the potent inhibitor **DMQCd** (Figure 1) could not be isolated. Furthermore, the amides **QCe**–**h** and **DMQCe**–**g** suffer from poor solubility, hampering full NMR spectroscopic analysis. The phenyl and adamantyl derivatives of the most active and effective carborane-based compounds were generated as comparative mimetic structures. For the introduction of the *N*-phenyl moiety and preparation of the phenylated quinazolin-4-amines (**QPc** and **DMQPa**–**d**), a copper-catalyzed Ullmann-type reaction of

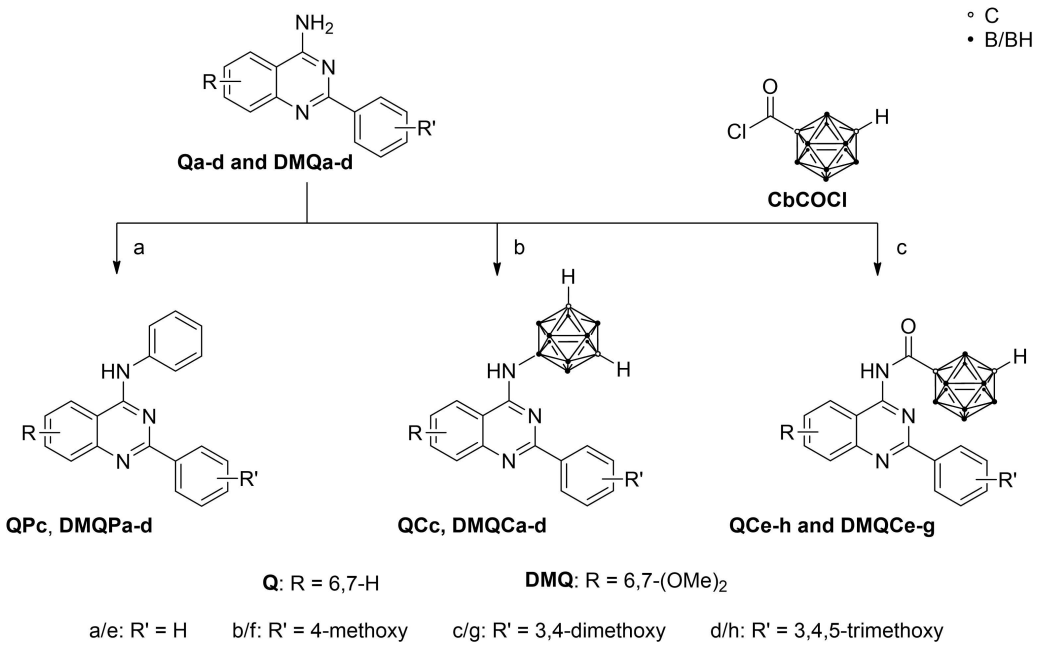

Scheme 1. General synthesis of *N*-substituted 2-phenylquinazolin-4-amine derivatives. Reagents and conditions: (a) iodobenzene, CuI, DMF, 130 °C; (b) *closo*-9-Br-1,7-dicarbadodecaborane,[17] SPhos Pd G4, SPhos, KO^{t}Bu, 1,4-dioxane, 80 °C, 1–2 h; (c) NEt_3, THF.

amines **Qc** and **DMQa**–**d** and iodobenzene was employed (Scheme 1a). The synthesis of *N*-carboranyl quinazolin-4-amines **QCc** and **DMQCa**–**d** was reported recently.[14]

In contrast, the adamantyl analogues (**QAc** and **DMQAa**–**d**) were not accessible via the quinazolin-4-amine intermediate, but were obtained by reacting adamantyl amine with 4-chloroquinazolines (**Cl-Qc** and **Cl-DMQa**–**d**, Scheme 2, b). The latter were obtained by reacting anthranilamide (**1**) or 4,5-dimethoxyanthranilamide (**2**) with substituted benzaldehydes **3**–**6** in EtOH in the presence of iodine to give the intermediate 2-substituted quinazolinones, which were reacted without further purification with excess $POCl_3$ to obtain the chlorinated compounds.

The phenyl and adamantyl derivative of **QCe** (**QPe** and **QAe**, respectively) were prepared in a similar manner to its carboranyl analogue, by reacting the appropriate phenyl- or adamantanyl-1-carbonyl chloride (**PhCOCl** or **AdmCOCl**) with 2-phenylquinazolin-4-amine (**Qa**) in the presence of triethylamine (Scheme 3).

All synthesized compounds were characterized by ^{1}H-NMR, ^{11}B-NMR (for carboranyl analogues), ^{13}C-NMR, 2D-NMR, IR spectroscopy and HR-MS, and purity was confirmed by elemental analysis (see the Supporting Information (SI)).

Biological investigation of the carboranyl amides (QCe–h and DMQe–g)

In preparation for the biological studies, the solubility in DMSO and in aqueous solution containing 0.5% DMSO was tested. The previously reported ABCG2-inhibiting quinazoline amines **QCc** and **DMQCa**–**d** exhibited no solubility problems and were used in concentrations > 25 μM in biological investigations.[14] However, for the corresponding quinazoline amides **QCf**–**h** and **DMQe**–**g** significant solubility issues were encountered. Only for compound **QCe**, the required concentrations could be reached, whereas with the introduction of further substituents in

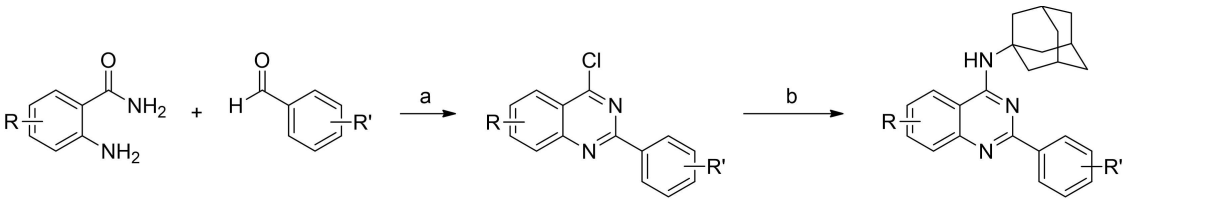

Scheme 2. Reagents and conditions: (a) i: I_2, EtOH, reflux; ii: $POCl_3$, reflux; (b) Adm-NH_2, Cs_2CO_3, 1,4-dioxane or DMF, 110 °C.

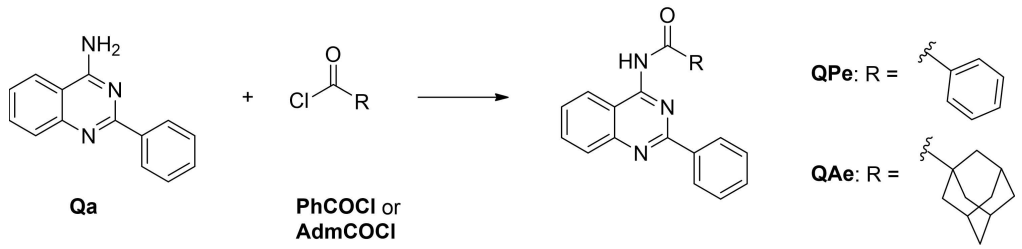

Scheme 3. Reagents and conditions: NEt_3, THF, reflux, 2 h.

compounds **QCf**–**h** and **DMQe**–**h**, the solubility decreased dramatically and the necessary concentrations for biological studies could not be achieved. Solubilizing substances, such as cyclodextrins (α- and β-cyclodextrin, 2-hydroxypropyl-β-cyclodextrin), used for highly hydrophobic agents to prevent aggregation or precipitation upon application, are known to improve the solubility of carborane-based compounds.[18] However, the poor solubility of **QCf**–**h** and **DMQe**–**g** still persisted even with the addition of these solubilizing agents. Moreover, in order to prove the full solubilization of **QCe** in an aqueous system and to exclude nanoparticle formation, Nanoparticle Tracking Analysis (NTA; **QCe** (50 μM) in 0.5% DMSO in water) was performed, revealing no formation of **QCe** nanoparticles within the tested particle size range (50 to 500 nM).

Determination of the cytotoxicity of QCe in MDCKII-hABCG2 and MDCKII wild-type cells

Due to low solubility of the amide derivatives, only **QCe** was selected for further biological testing. The cytotoxicity of **QCe** on wild-type Madin-Darby canine kidney (MDCKII-WT) and human ABCG2-transfected MDCKII cells (MDCKII-hABCG2) was investigated in a WST-1 (4-[3-(4-iodophenyl)-2-(4-nitro-phenyl)-2*H*-5-tetrazolio]-1,3-benzene sulfonate) cell proliferation assay. DMSO (0.1%) and Triton X-100 were used as negative and positive control, respectively. Compound **QCe** exhibited no significant cytotoxicity up to 25 μM in both cell lines (SI, Figure S101A). No IC_{50} value could be obtained above 25 μM due to low solubility.

Hoechst 33342 assay-based evaluation of the inhibitory potential of QCe toward MDCKII-hABCG2 cells

The ability of compound **QCe** to inhibit the ABCG2 transporter was investigated on human ABCG2-overexpressing MDCKII-hABCG2 cells in a Hoechst 33342 assay as previously reported.[14] Inhibition of the BCRP-mediated transport of Hoechst 33342, a fluorescent dye and BCRP substrate, leads to accumulation of the dye within the cell. An increased intracellular Hoechst concentration reflects an ABCG2 inhibition. Ko143 (Figure 1A), an ABCG2 inhibitor and standard reference, was used as positive control; DMSO (0.1%) was used as negative control. **QCe** was applied in concentrations between 0.05 and 1.0 μM, in order to assess lower micromolar and submicromolar inhibition (Figure 3). In comparison to its *N*-carboranyl amine derivative **QCa**,[14] the unsubstituted *N*-(*meta*-carboran-1-oyl)-2-phenylquinazolin-4-amine **QCe** exhibited significant inhibition of ABCG2 at 0.5 and 1.0 μM. The beneficial effect of the amide linker may be due to the increased flexibility. This is in agreement with the findings of Wiese and co-workers, indicating similar improvement of the inhibitory activity of the *N*-benzoylquinazolin-4-amine compared to its *N*-phenyl analogue.[19]

Comparative evaluation of the cytotoxicity of the most promising compounds and their phenyl and adamantyl analogues

The previously reported compounds *N*-(*meta*-carboran-9-yl)-2-phenylquinazolin-4-amines **DMQCc** and **DMQCd** and the *N*-(*meta*-carboran-1-oyl)-2-phenylquinazolin-4-amine **QCe** reported here were identified as the most promising candidates for further investigations. Carboranes are often used as phenyl mimetics to improve the metabolic stability and affinity towards different targets by increased electronic interactions with the boron-based cluster.[10] Therefore, the phenyl analogues (**QPe**, **DMQPc**, and **DMQPd**; Schemes 1, a and 3) were synthesized

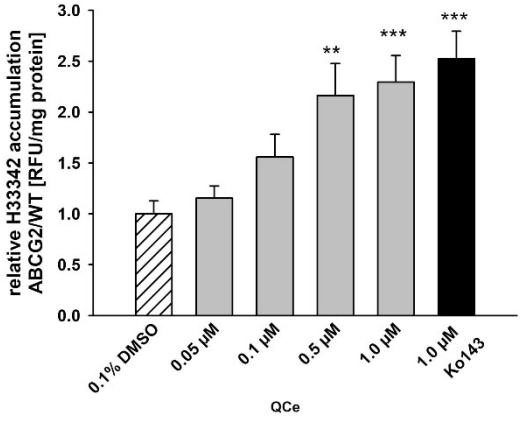

Figure 3. Intracellular Hoechst 33342 accumulation in MDCKII-hABCG2 cell in comparison to MDCKII-WT cells. Cells were treated with **QCe** or the positive control Ko143. Data were normalized to solvent control (0.1% DMSO) and are presented as mean ± SEM of five independent experiments (N = 5, one-way ANOVA with Holm-Šidák post hoc test, * significant difference in comparison to solvent control: *** $p \leq 0.001$, ** $p \leq 0.01$).

and included in this study. Furthermore, the corresponding adamantyl analogues (**QAe**, **DMQAc**, and **DMQAd**; Schemes 2 and 3) were prepared to elucidate whether the mode of action is influenced by steric or electronic effects, or both. The cytotoxicity of the *N*-phenyl- and *N*-adamantylquinazoline amines and amides (**QPe**, **QAe**, **DMQPc**, **DMQAc**, **DMQPd** and **DMQAd**) was determined by a WST-1 cell proliferation assay in MDCKII-hABCG2 and their parental MDCKII-WT cells, as mentioned above. Obtained half-maximal inhibition concentration (IC_{50}) of each compound is given in Table 1. The *N*-phenyl- and *N*-adamantylquinazoline amines and amides were compared to the most promising carboranyl analogues **QCe** and recently reported[14] **DMQCc** and **DMQCd**. Due to limited solubility, the highest concentration of the stock solution was 50 mM and concentrations below 50 μM were applied. For **QCe**, the highest available concentration of 25 mM was used as stock solution. In comparison to the carboranyl derivatives, lower solubility of the organic analogues **QAe**, **QPe**, **DMQAc**, **DMQPc**, and **DMQPd** was observed. In the case of the phenyl and the adamantyl derivative of **QCe** (**QPe** and **QAe**, respectively), a concentration range of up to 5 and 10 μM, respectively, was tested. While **QCe** caused a slightly decreased cell viability at 25 μM, no IC_{50} value could be obtained for the three compounds (SI, Figure S101A, B, C). However, in the case of compound **DMQCc** and its organic analogues **DMQAc** and **DMQPc**, solubility difficulties were evident (highest applied concentration 25 μM), yet both organic derivatives showed significantly lower IC_{50} values compared to the carborane analogue **DMQCc** ($IC_{50} \geq 50$ μM[14]). In particular, compound **DMQPc** exhibited enhanced toxicity with IC_{50} values in lower micromolar ranges (IC_{50}~1.9 μM; for both cell lines, Figure S102B). The adamantyl derivative **DMQAc** further showed cell line-specific cytotoxicity (Table 1; SI, Figure S102A). The IC_{50} value against MDCKII-hABCG2 cells is approximately half the value compared to its parent cell line MDCKII-WT (IC_{50} = 9.79 and 23.41 μM, respectively). Similar effects were observed for the adamantyl derivative **DMQAd** of compound **DMQCd** (**DMQAd**: IC_{50} MDCKII-hABCG2 = 9.42 μM, IC_{50} MDCKII-WT = 42.81 μM; **DMQCd**: IC_{50} for both cell lines ≥ 50 μM[14]). As the phenyl derivative **DMQPd** exhibited very low solubility, a concentration-effect curve up to only 1 μM could be assessed (SI, Figure S103B). Hence, regarding their cytotoxicity, the carborane compounds exhibit significant advantages over their organic analogues. Moreover, low toxicity of the carboranyl amines **DMQCc** and **DMQCd** was observed compared to their phenyl and adamantyl analogues.

Evaluation of the inhibitory activity against MDCKII-hABCG2 cells in Hoechst 33342 accumulation assay

The Hoechst 33342 accumulation assay was used to determine the inhibitory activity of the adamantyl and phenyl analogues **QAe**, **QPe**, **DMQAc**, **DMQPc**, **DMQAd** and **DMQPd** in comparison to the carboranyl derivatives (**QCe**, **DMQCc** and **DMQCd**) towards human ABCG2. Investigation of the ability to inhibit the human ABCG2 transporter in MDCKII-hABCG2 cells followed the procedure as previously described.[14] Since no cytotoxic effects were observed below 1 μM, the tested compounds were administered in concentrations of 0.5 and 1.0 μM. Ko143 was added as positive control (1.0 μM).

As shown in Figures 3 and 4A, **QCe** inhibited the human ABCG2 efflux activity at both concentrations, 0.5 μM and 1 μM, while the adamantyl analogue exhibited no inhibition, and the phenyl analogue revealed strong inhibitory activity (Figure 4A). The results of the phenyl analogue **QPe** are consistent with previous reports by Krapf et al..[19] Concerning the comparative structures of the tetra-methoxylated compounds **DMQCc**, **DMQAc** and **DMQPc**, no BCRP inhibition at any applied concentration was detected (Figure 4B). As reported previously,[14] **DMQCc** exhibited autofluorescence which did not allow determination of inhibition in the Hoechst accumulation assay. Consequently, for compounds **DMQAc** and **DMQPc**, autofluorescence measurements were performed to exclude any influence of increased fluorescence background values on

Table 1. Cytotoxicity of compounds **QCe**, **DMQCc**, **DMQCd** and their adamantyl (**QAe, DMQAc, DMQAd**) and phenyl analogues (**QPe, DMQPc, DMQPd**) (Q = quinazoline scaffold; DMQ = 6,7-dimethoxyquinazoline scaffold; specification of amine or amide-bound moiety: **C** = carboranyl; **A** = adamantyl; **P** = phenyl) determined by WST-1 cell proliferation assay using MDCKII wild-type (MDCKII-WT) and human ABCG2-transfected MDCKII cells (MDCKII-hABCG2). Data given as mean ± SEM of three independent experiments (N = 3). n.t. = not tested.

	Compound	R	R′	N-substituent	IC_{50} ± SEM [μM] MDCKII-WT	IC_{50} ± SEM [μM] MDCKII-hABCG2
Amide derivatives	**QCe**	H	H	1-carboranyl	>25[a]	>25[a]
	QAe	H	H	1-adamantyl	>10[b]	>10[b]
	QPe	H	H	phenyl	>5[c]	>5[c]
Amine derivatives	**DMQCc**	6,7-$(OMe)_2$	3,4-$(OMe)_2$	carboran-9-yl	>50[14]	>50[14]
	DMQAc	6,7-$(OMe)_2$	3,4-$(OMe)_2$	1-adamantyl	23.41 ± 0.16	9.79 ± 0.16
	DMQPc	6,7-$(OMe)_2$	3,4-$(OMe)_2$	phenyl	1.88 ± 0.14	1.83 ± 0.14
	DMQCd	6,7-$(OMe)_2$	3,4,5-$(OMe)_3$	carboran-9-yl	>50[14]	>50[14]
	DMQAd	6,7-$(OMe)_2$	3,4,5-$(OMe)_3$	1-adamantyl	42.81 ± 0.15	9.42 ± 0.14
	DMQPd	6,7-$(OMe)_2$	3,4,5-$(OMe)_3$	phenyl	>1[d]	>1[d]

[a] Highest applied concentration 25 μM, due to poor solubility in DMSO; [b] highest applied concentration 10 μM, due to poor solubility in DMSO; [c] highest applied concentration 5 μM, due to poor solubility in DMSO; [d] highest applied concentration 1 μM, due to poor solubility in DMSO.

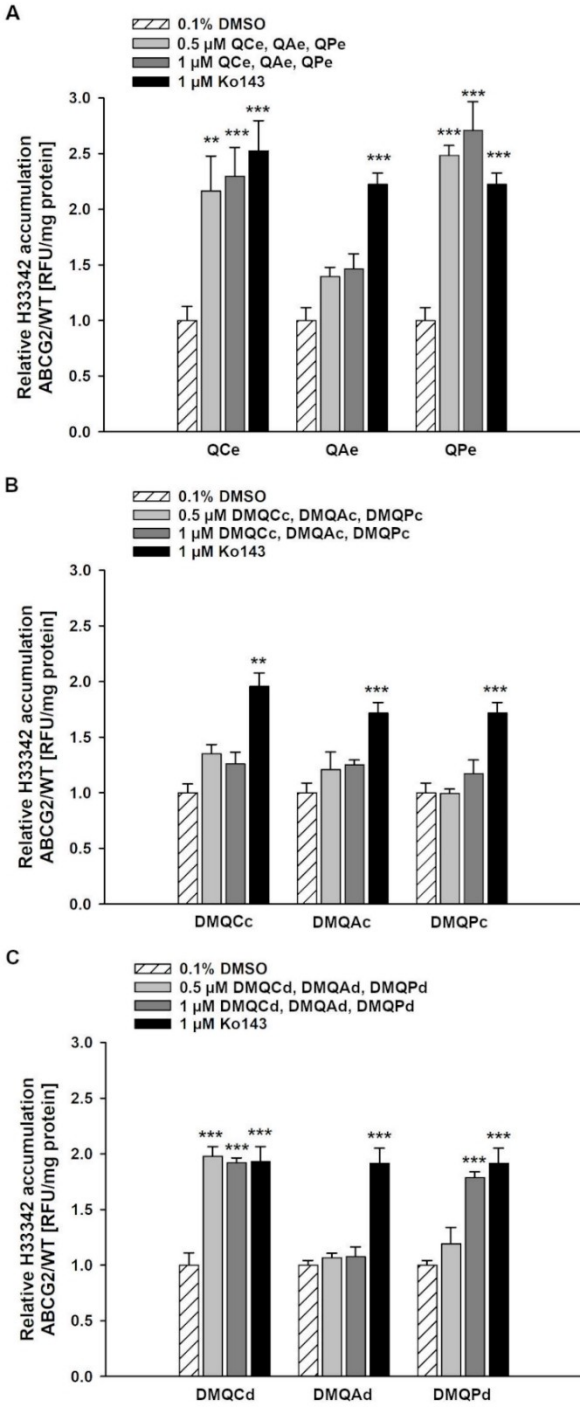

Figure 4. Intracellular Hoechst 33342 accumulation in MDCKII-hABCG2 cells in comparison to MDCKII-WT cells. Cells were treated with (**A**) **QCe**, **QAe**, **QPe**, (**B**) **DMQCc**, **DMQAc**, **DMQPc**, and (**C**) **DMQCd**, **DMQAd**, **DMQPd** or the positive control Ko143. Data were normalized to solvent control (0.1% DMSO) and are presented as mean ± SEM of five independent experiments (N = 5, one-way ANOVA with Holm-Šidák post hoc test, * significant difference in comparison to solvent control: *** $p \leq 0.001$, ** $p \leq 0.01$, * $p \leq 0.05$). Data of **DMQCc** and **DMQCd** were taken from our previous study.[14]

the obtained data. Investigating the influence of exchanging the carboranyl moiety with phenyl or adamantyl for the, so far, most potent carboranyl quinazoline compound **DMQCd** revealed remarkable differences. Compound **DMQCd** significantly inhibited the ABCG2 transporter in lower concentrations than **DMQPd**, while showing no significant inhibition at 0.5 µM (Figure 4C). Surprisingly, the adamantyl derivative **DMQAd** yielded no inhibitory activity at both tested concentrations (Figure 4C), suggesting either autofluorescence effects as found for other investigated compounds, or the advantages of the carborane as a pharmacophore.

Determination of autofluorescence of QCe, QAe, and QPe

Compounds may exhibit autofluorescence, leading to an underestimation of ABCG2 interaction determined by Hoechst 33342 accumulation assay. Therefore, the degree of autofluorescence of compounds **QCe**, **QAe**, and **QPe** in 0.5 and 1.0 µM in comparison to the reference Ko143 (1.0 µM) was assessed as described previously.[20] No autofluorescence was detected for **QCe**, **QAe** or **PQe** in MDCKII-hABCG2 (SI, Figure S104A) and MDCKII-WT cells (SI, Figure S104B). As previously reported for **DMQCc**,[14] **DMQAc** is also autofluorescent in both cell lines while **DMQPc** is not (SI, Figure S105). Thus, **DMQAc** may also inhibit ABCG2 but is not detectable by Hoechst 33342 accumulation assay. Similar to **DMQCc**, **DMQCd** and **DMQAd** exhibit autofluorescence (SI, Figure S106). Again, the phenyl analogue **DMQPd** showed no increased intracellular fluorescence by itself (SI, Figure S106). Overall, the influence of the autofluorescent carboranyl and adamantyl analogues on ABCG2 inhibition in the Hoechst 33342 accumulation assay may be underestimated. Thus, all investigated compounds were included in the mitoxantrone (MXN) reversal study in MDCKII-hABCG2 cells.

Investigation of ABCG2-mediated mitoxantrone-resistance reversal in MDCKII-hABCG2 cells

Recently, a meta-analysis surveying different studies was published looking at the expression of ABC transporters in over 50,000 patients,[21] with ABCG2 being expressed in 66% of the cases; co-expression of all three ABC proteins was found in 29% of the patients. However, clinical failure of chemotherapies and poor survival remains a major obstacle due to the overexpression of these ABC transporters and, consequently, the occurrence of resistance to clinically used therapeutic agents, such as mitoxantrone (MXN).[22]

Considering the ability of the tested compounds to inhibit the ABCG2 transporter, we investigated whether co-administration of the inhibitors reverse the ABCG2-mediated mitoxantrone resistance in ABCG2-overexpressing cells (MDCKII-hABCG2). MXN has been identified as a substrate of BCRP and is actively transported out of the cell in an accelerated and increased manner due to overexpression of the ABC transporter.[23]

Successful inhibition of ABCG2 results in enhancement of MXN efficacy by increasing intracellular MXN amount, and thus, potentially leads to a reversal of MDR. The inhibitors of human ABCG2, chosen for their high inhibitory activity in the Hoechst

assay (**QCe**, **DMQCc**, **DMQCd**), and their organic analogues (**QAe**, **QPe**, **DMQAc**, **DMQPc**, **DMQAd**, **DMQPd**) were selected for investigation in co-administration with MXN. A successful reversal of ABCG2-mediated MXN resistance is reflected by a left-shift in the concentration-effect curve of MXN with inhibitor in comparison to MXN alone. Obtained IC_{50} values and corresponding left-shift factors, as well as prior results as comparison,[14] are given in Table 2 and Figures 5–7.

Previously, we have shown the significant increase of the IC_{50} value of MXN in human ABCG2-overexpressing cell lines (MDCKII-hABCG2) compared to the parental cell line MDCKII-WT, namely 2.649 ± 0.594 μM and 0.519 ± 0.042 μM, respectively, substantiating the BCRP-mediated decrease in MXN toxicity.[20] As the Hoechst 33342 inhibition studies indicated, a similar trend was found in the MDR-reversal studies. The carboranyl analogue **QCe** (Figure 5A) and phenyl analogue **QPe** (Figure 5C) caused a significant strong left-shift of the MXN-concentration-effect curve in comparison to MXN alone while its adamantyl analogue did not (Figure 5B). Within the second set of tested compounds, all tetra-methoxylated derivatives (**DMQCc**, **DMQAc** and **DMQPc**, Figure 6) showed the ability to reverse the ABCG2-mediated resistance. The highest significant left-shift (about 9.8-fold) was obtained for the carboranyl quinazoline derivative **DMQCc**.[14] Surprisingly, the Hoechst studies revealed no significant inhibition of hABCG2 for the three tested compounds (Figure 4) which might be caused by autofluorescence. Finally, the superiority of carboranyl quinazoline derivative **DMQCd** among the three penta-methoxylated derivatives validated the observed strongest inhibitory activity in the Hoechst assay. The addition of the phenyl and adamantyl analogues **DMQPd** (Figure 7B) and **DMQAd** (Figure 7A) yielded reduced IC_{50}(MXN) values of 0.364 ± 0.063 and 0.273 ± 0.056 μM, respectively, resulting in left-shifts of 4.6- and 5.9-fold, respectively. Reversal of resistance was observed for the adamantyl derivative **DMQAd**, which exhibited no inhibition in the Hoechst studies. As shown in Figure 4, the intracellular Hoechst 33342 fluorescence appears to be superimposed on

Table 2. Left-shift factor calculated as IC_{50} MXN/IC_{50} MXN in combination with quinazoline derivatives determined in MDCKII-hACBG2 cells using WST-1 assay. IC_{50} values are given as mean ± SEM (N = 3, two-way ANOVA, * represents significant difference in comparison to single MXN treatment, * < 0.05, ** p < 0.01; *** p < 0.001).

Treatment of MDCKII-hABCG2	IC_{50} [μM]	Left-shift factor	Comparison to MXN*
MXN	2.649 ± 0.594		
MXN + 1 μM **QCe**	1.109 ± 0.168	1.6-fold	**
MXN + 1 μM **QAe**	1.451 ± 0.239	1.2-fold	
MXN + 1 μM **QPe**	0.880 ± 0.083	2.1-fold	***
MXN + 1 μM **DMQCc**	0.184 ± 0.025[14]	9.8-fold	***
MXN + 1 μM **DMQAc**	0.297 ± 0.049	6.0-fold	***
MXN + 1 μM **DMQPc**	0.512 ± 0.033	3.6-fold	***
MXN + 1 μM **DMQCd**	0.144 ± 0.033[14]	11.6-fold	***
MXN + 1 μM **DMQAd**	0.364 ± 0.063	4.6-fold	**
MXN + 1 μM **DMQPd**	0.273 ± 0.056	5.9-fold	*

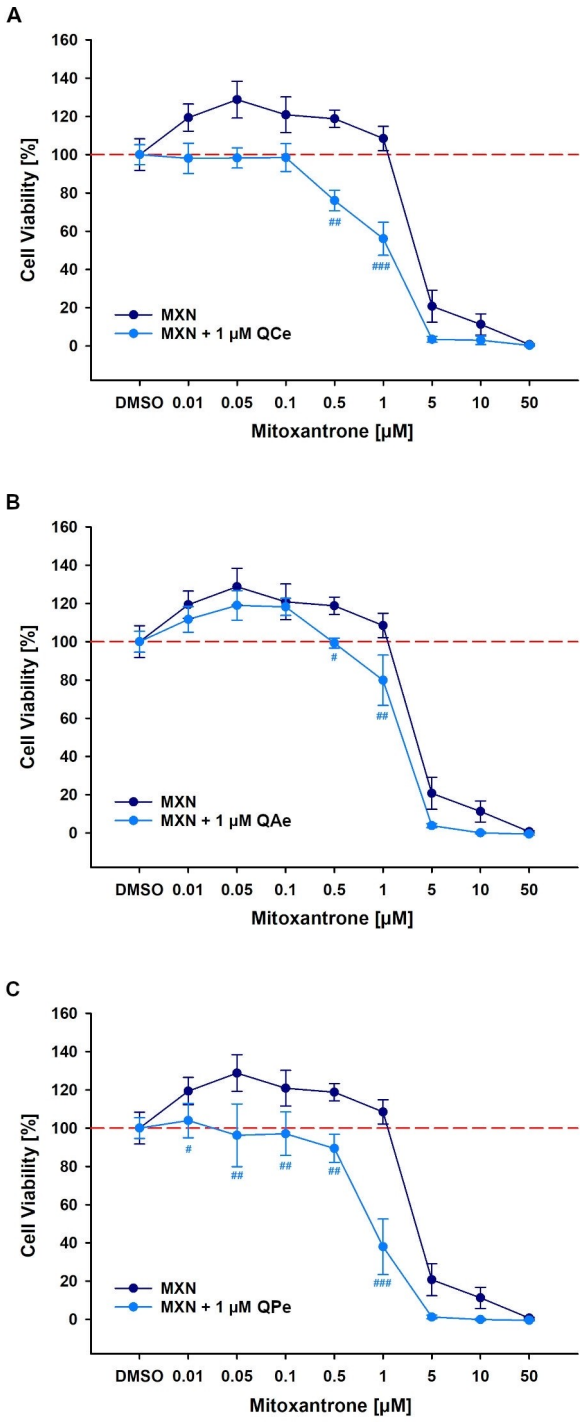

Figure 5. Reversal of MXN resistance in MDCKII-hABCG2 cells by 1 μM of (**A**) **QCe**, (**B**) **QAe**, and (**C**) **QPe**. MDCKII-hABCG2 cells were treated with MXN in increasing concentrations with or without 1 μM of the investigated compounds for 48 h. Afterwards, cell viability was assessed by WST-1 assay. Data were normalized to solvent control (0.1% DMSO) and are presented as mean ± SEM (N = 3, two-way ANOVA with Holm-Šidák post hoc test, # significant difference in comparison to MXN treatment alone: ### p ≤ 0.001, ## p ≤ 0.01, # p ≤ 0.05).

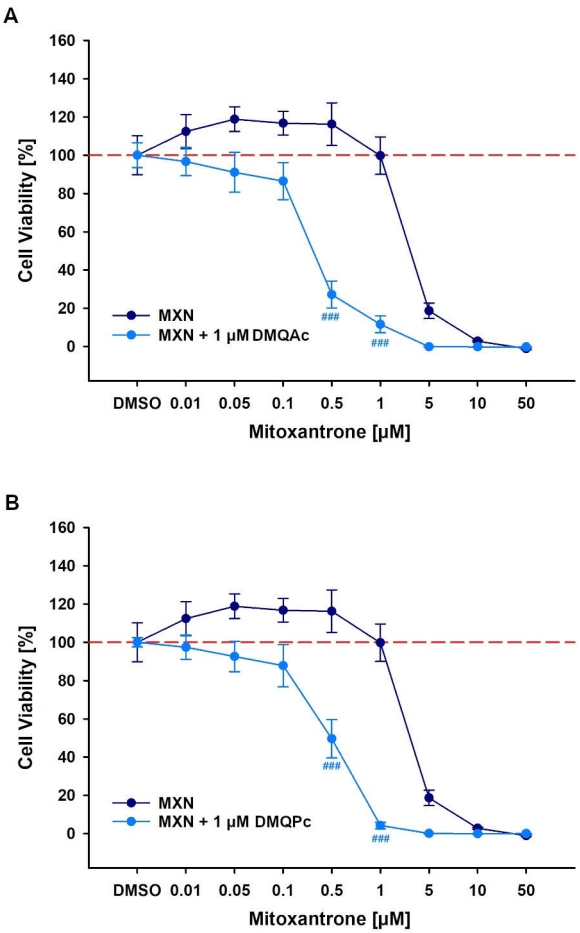

Figure 6. Reversal of MXN resistance in MDCKII-hABCG2 cells by 1 µM of (**A**) **DMQAc** and (**B**) **DMQPc** (**DMQCc** was presented previously[14]). MDCKII-hABCG2 cells were treated with MXN in increasing concentrations with or without 1 µM of the investigated compounds for 48 h. Afterwards, cell viability was assessed by WST-1 assay. Data were normalized to solvent control (0.1 % DMSO) and are presented as mean ± SEM (N = 3, two-way ANOVA with Holm-Šidák post hoc test, # significant difference in comparison to MXN treatment alone: ### $p \leq 0.001$, ## $p \leq 0.01$, # $p \leq 0.05$).

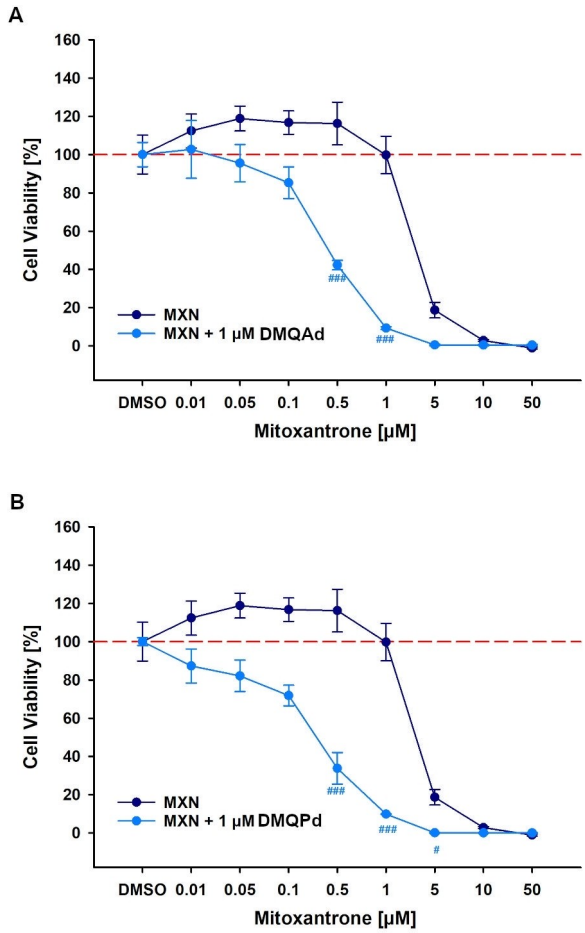

Figure 7. Reversal of MXN resistance in MDCKII-hABCG2 cells by 1 µM of (**A**) **DMQAd** and (**B**) **DMQPd** (for **DMQCd** see Stockmann et al.[14]). MDCKII-hABCG2 cells were treated with MXN in increasing concentrations with or without 1 µM of the investigated compounds for 48 h. Afterwards, cell viability was assessed by WST-1 assay. Data were normalized to solvent control (0.1 % DMSO) and are presented as mean ± SEM (N = 3, two-way ANOVA with Holm-Šidák post hoc test, # significant difference in comparison to MXN treatment alone: ### $p \leq 0.001$, ## $p \leq 0.01$, # $p \leq 0.05$).

the autofluorescence of **DMQAd** (SI, Figure S106). However, the administration of penta-methoxy carboranyl quinazoline derivative **DMQCd**[14] significantly exceeded both its organic analogues, decreasing the IC_{50} value of mitoxantrone to 0.144 ± 0.033 µM, representing a left-shift factor of 11.6. In consequence, the *N*-carboranyl quinazolin-4-amines **DMQCc** and **DMQCd** were able to reverse BCRP-mediated mitoxantrone resistance in MDCKII-hABCG2 cells, outperforming their organic phenyl and adamantyl analogues.

Investigation of mitoxantrone-resistance in HT29 colon cancer cells

The MDCKII-hABCG2 cell line is a transfected cell line originated from canine kidney. As known from other cell lines, cancer cells exhibit a different expression of transporters and metabolic enzymes than non-cancer cell lines.[24] Thus, human colorectal adenocarcinoma cell line HT29 with a comparable high intrinsic ABCG2 expression[24] was used to prove whether the investigated compounds are able to reverse MXN-mediated drug resistance similar as described for MDCKII-hABCG2 cells. **QCe**, **QAe**, and **QPe** demonstrated the lowest solubility and the lowest left-shift factor in MDCKII-hABCG2 cells; MXN reversal studies in HT29 cells were, therefore, only performed for **DMQCc**, **DMQCd** and their respective phenyl and adamantyl analogues (Figures 8 and 9). Table 3 presents the IC_{50} values and calculated left-shift factors.

Overall, MXN caused a higher toxicity towards HT29 cells than towards MDCKII-hABCG2 cells, with IC_{50} values of about 0.657 ± 0.165 µM and 2.649 ± 0.594 µM, respectively. Therefore, lower left-shift factors were calculated for HT29 cells than the ones presented for MDCKII-hABCG2 cells. The reference compound Ko143 did not lead to a significant left-shift of the MXN concentration-effect curve in the applied concentration (SI, Figure S107). Of the tetra-methoxylated derivatives **DMQCc**, **DMQAc** and **DMQPc**, only the carboranyl and adamantyl analogues reversed the MXN resistance in HT29 cells in a

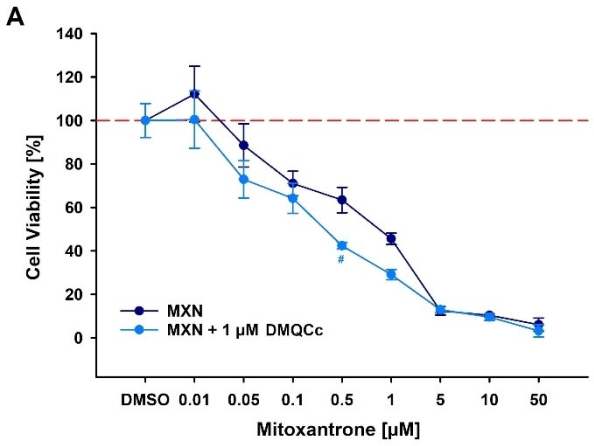

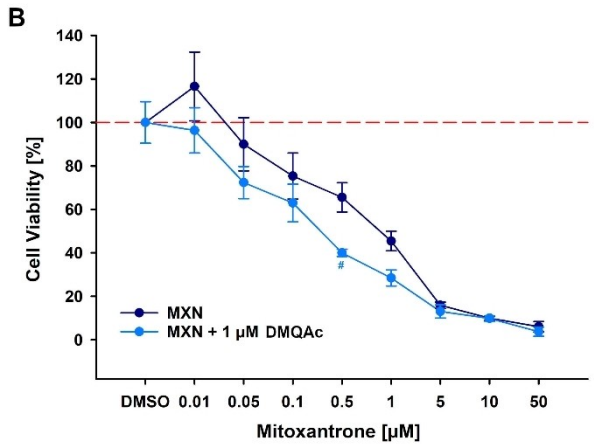

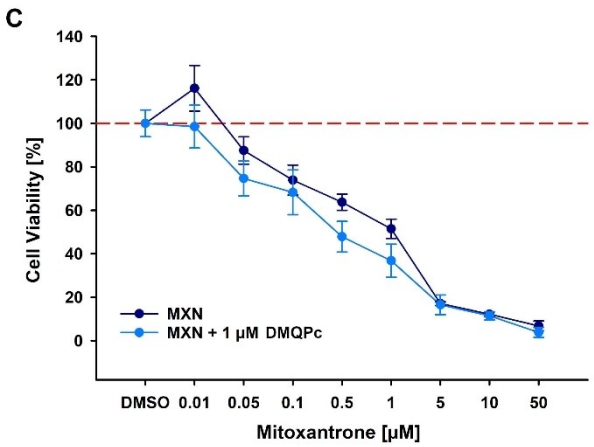

Figure 8. Reversal of MXN resistance in HT29 colon adenocarcinoma cells. Cells were treated with increasing concentrations of MXN and with 1 µM of (**A**) **DMQCc**, (**B**) **DMQAc** and (**C**) **DMQPc** for 48 h. Afterwards, cell viability was assessed by MTT assay. Data were normalized to solvent control (0.1% DMSO) and set as 100% (mean ± SEM, N = 3, two-way ANOVA with Holm-Šidák post hoc test, #significant difference in comparison to the MXN treatment alone: ### $p \leq 0.001$, ## $p \leq 0.01$, # $p \leq 0.05$).

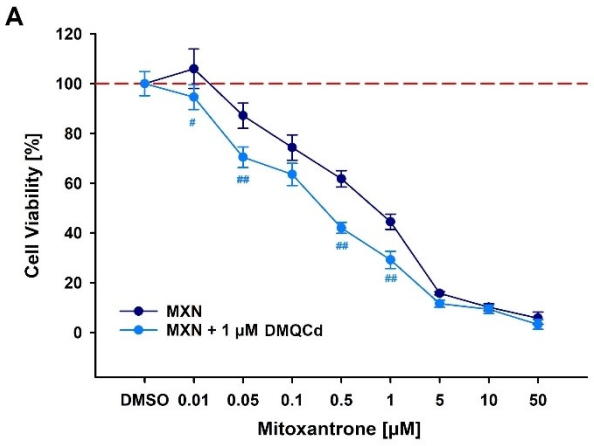

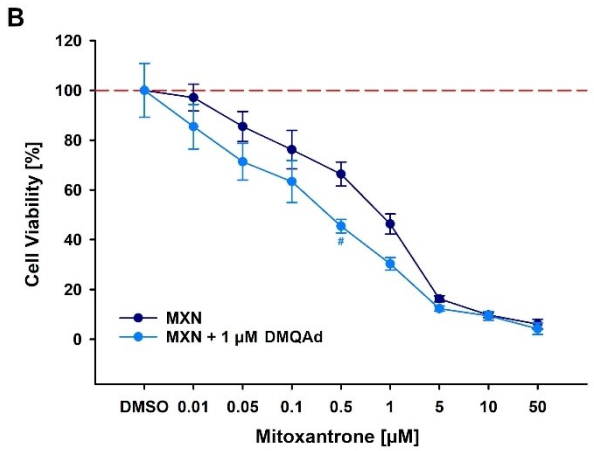

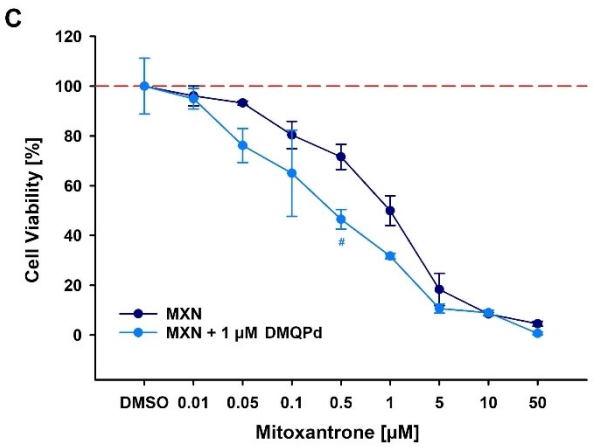

Figure 9. Reversal of MXN resistance in HT29 colon adenocarcinoma cells. Cells were treated with increasing concentrations of MXN and with 1 µM of (**A**) **DMQCd**, (**B**) **DMQAd**, and (**C**) **DMQPd** for 48 h. Afterwards, cell viability was assessed by MTT assay. Data were normalized to solvent control (0.1% DMSO) and set as 100% (mean ± SEM, N = 3, two-way ANOVA with Holm-Šidák post hoc test, #significant difference in comparison to the MXN treatment alone: ### $p \leq 0.001$, ## $p \leq 0.01$, # $p \leq 0.05$).

significant manner with a left-shift factor of 1.2 (Table 3; Figure 8). Similar as shown by MDCKII-hABCG2 cells, phenyl analogue **DMQPc** caused the lowest reversal of MXN resistance, which is in line with the results of the MDCKII-hABCG2 cells. Therefore, the undetectable interaction of **DMQPc** in the Hoechst 33342 accumulation assay might be attributed to a low level of ABCG2 inhibition below the detection limit.

DMQCd and its organic analogues **DMQAd** and **DMQPd** were able to reverse MXN drug resistance in HT29 cancer cells with a left-shift factor of about 1.6, 1.3 and 1.7, respectively

Table 3. Left-shift factor calculated as IC_{50} MXN/IC_{50} MXN in combination with quinazoline derivatives determined in colorectal adenocarcinoma cells HT29 using MTT assay. IC_{50} values are given as mean ± SEM (N = 3, two-way ANOVA, * represents significant difference in comparison to single MXN treatment, * < 0.05, ** $p < 0.01$; *** $p < 0.001$).

Treatment of HT29	IC_{50} [μM]	Left-shift factor	Comparison to MXN*
MXN	0.657 ± 0.165		
MXN + 1 μM Ko143	0.559 ± 0.130	0.7-fold	
MXN	0.628 ± 0.264		
MXN + 1 μM **DMQCc**	0.232 ± 0.082	1.2-fold	*
MXN	0.658 ± 0.315		
MXN + 1 μM **DMQAc**	0.213 ± 0.073	1.2-fold	**
MXN	0.728 ± 0.305		
MXN + 1 μM **DMQPc**	0.375 ± 0.175	0.8-fold	*
MXN	0.670 ± 0.188		
MXN + 1 μM **DMQCd**	0.232 ± 0.082	1.6-fold	***
MXN	0.907 ± 0.307		
MXN + 1 μM **DMQAd**	0.310 ± 0.141	1.3-fold	**
MXN	1.133 ± 0.291		
MXN + 1 μM **DMQPd**	0.350 ± 0.147	1.7-fold	**

(Table 3; Figure 9). Moreover, the significantly increased potential of compound **DMQCd** to reverse MXN resistance in ABCG2-overexpressing MDCKII cells in comparison to reference Ko143 can potentially be explained by different affinities of the compounds toward the ABCG2 transporter.[25]

In silico investigations – molecular docking simulations and investigation of mode of inhibition

As the mechanism of BCRP is not fully understood,[26] for a better understanding of putative binding modes of the inhibitors, the nine biologically investigated compounds **QCe**, **QAe**, **QPe**, **DMQCc**, **DMQAc**, **DMQPc**, **DMQCd**, **DMQAd**, and **DMQPd** were screened by computational methods on the cryo-electron microscopy (EM) structure of the human ABCG2 transporter protein.[27] For this purpose, the structures of the phenyl, adamantyl and carboranyl quinazoline compounds were docked into the crystal structure of the protein to reveal and evaluate probable binding modes and substrate-receptor interactions. Molecular structures as well as the protein structure were prepared according to published methods.[14] In previous studies, as well as in the literature, the binding behavior of Hoechst 33342 was studied, which is found in a more lateral binding pocket in the inner cavity of the transporter (binding pocket S2[19]). However, our studies showed a total occupancy of the inner binding pocket S1 by the investigated compounds. Furthermore, a comparison of the respective phenyl, adamantyl and carboranyl structures showed similar binding behavior, with similar orientations as well as interactions between substrate and protein, as exemplified in Figure 10 for **DMQCd**, **DMQAd** and **DMQPd**. We have demonstrated a similar binding pose of **DMQCd** in previous work,[14] which resembles the co-crystallized structure of the inhibitor MZ29 with BCRP[28] or the structure of MXN:BCRP.[29] Similarly, the quinazoline moiety of the phenyl and adamantyl derivative forms a strong $\pi - \pi$ stacking interaction between the opposed phenylalanine residues (Phe439) of both monomers. Moreover, hydrophobic as well as donor-acceptor interactions between the methoxy groups and the protonated asparagine residue Asn436 are present. However, comparison of the binding modalities among the examined structures suggests a non-competitive behavior towards Hoechst 33342 and a more competitive behavior towards MXN, due to occurring occupancy in similar or different binding pockets, respectively.

Conclusions

The relevance of carboranes as pharmacophores in ABCG2 inhibitors in comparison to their phenyl as well as their sterically demanding, aliphatic adamantyl equivalents was evaluated, based on our previous work[14] and novel (polymethoxylated) *N*-carboran-1-oyl 2-phenylquinazoline amine derivatives. The unsubstituted derivative **QCe** exhibited comparably low toxicity and the ability to inhibit the human ABCG2 transporter in a Hoechst 33342 accumulation assay. However, the other carboranoyl derivatives evinced poor solubility, hampering further biological investigations.

As carboranes are often considered as three-dimensional mimics of phenyl rings, with exhibiting a higher steric demand and hydrophobicity like an adamantyl moiety, the associated phenyl and adamantyl analogues (**QAe**, **QPe**, **DMQAc**, **DMQPc**, **DMQAd** and **DMQPd**) of the best inhibitors (**QCe**, **DMQCc** and **DMQCd**) were synthesized. However, especially the phenyl derivatives showed low solubility, limiting the concentration ranges within the biological assessments to only 1 or 5 μM for **DMQPd** and **QPe**, respectively. Furthermore, the tetra-methoxylated derivative **DMQPc** showed the highest cytotoxicity among the tested compounds. Similarly, among the adamantyl derivatives, the tetra-methoxylated analogue exhibited the highest cytotoxicity, with the carboranyl analogue showing no toxicity below 50 μM. In general, the carboranyl quinazolines **QCe**, **DMQCc** and **DMQCd** demonstrated the best solubility and lowest cytotoxic effect within our investigations. The evaluation of inhibitory activity in Hoechst assays showed stronger inhibition by the phenyl analogue **QPe** compared to the carboranyl derivative **QCe**. This was in line with the MDR-reversal studies, where compound **QPe** gave the strongest left-shift (2.1-fold) in a combined application of inhibitor (1.0 μM) with mitoxantrone in comparison to its analogues.

The tetra-methoxylated derivatives indicated no significant inhibition of the human ABCG2 transporter due to autofluorescent behavior which was confirmed for **DMQCc** and **DMQAc**.

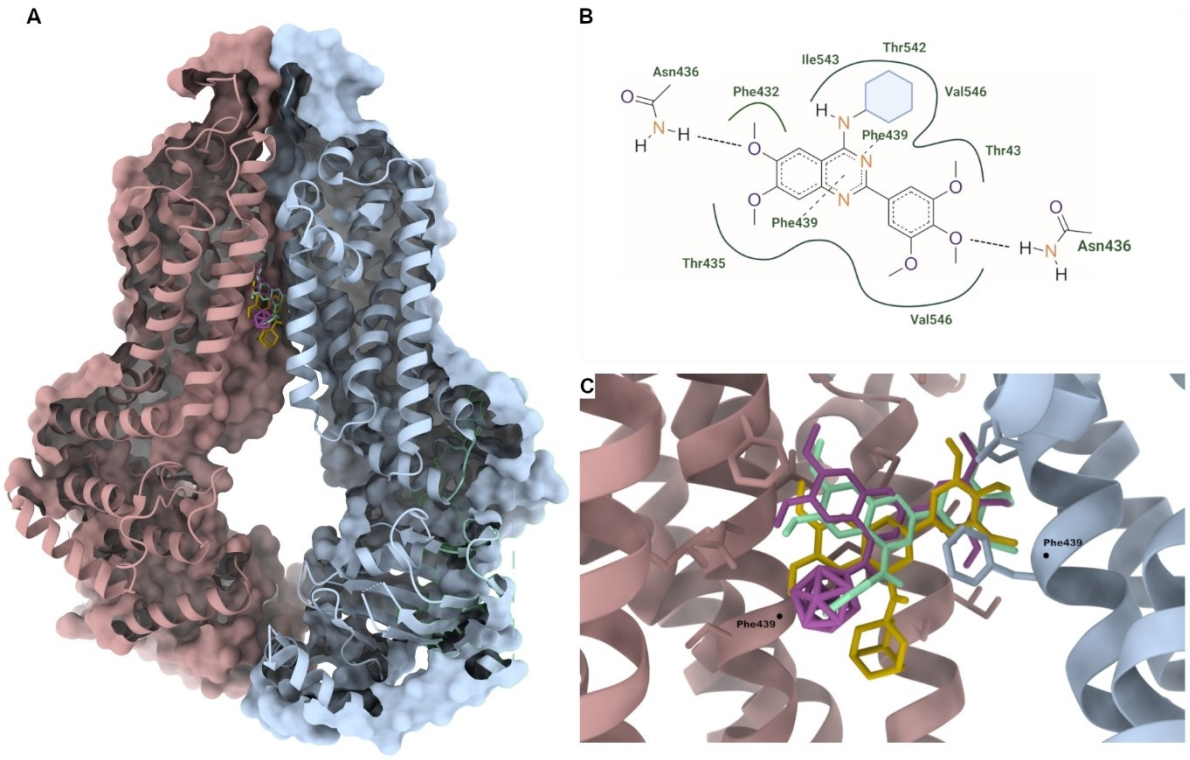

Figure 10. Cartoon representation of ABCG2 with monomers depicted in rose and blue; (**A**) top-ranked binding poses of **DMQCd** (pink), **DMQAd** (yellow) and **DMQPd** (green) within cavity S1.[19] (**B**) 2D interaction diagram of the top score poses of **DMQCd** and **DMQPd**; the blue hexagon represents the carboranyl or phenyl moiety. (**C**) Docking of **DMQCd**, **DMQAd** and **DMQPd** into the crystal structure of ABCG2 (5NJ3); structures shown as stick model; hydrogen atoms omitted for clarity; binding free energies: −8.1, −6.1 and −7.3 kcal/mol, respectively.

Both organic analogues **DMQAc** and **DMQPc** caused a strong reversal of MXN resistance, in contrast to the carboranyl derivative **DMQCc**. The organic penta-methoxy-substituted derivatives **DMQAd** and **DMQPd** showed no comparable potency in the Hoechst 3342 assays compared with the parental carboranyl derivative **DMQCd**. Similar as **DMQCc**, compound **DMQAd** exhibited autofluorescence leading to an underestimation of a potential ABCG2 inhibition. All compounds reversed mitoxantrone resistance in MDCKII-hABCG2 and HT29 colon cancer cells. Overall, all carborane-based derivatives exhibited higher solubility and lower toxicity as their phenyl and adamantyl analogues. Moreover, the most efficient MDR-reversing BCRP inhibitor was compound **DMQCd** which reversed MXN resistance in MDCKII-hABCG2 and HT29 colon cancer cells.

Experimental Section

Syntheses

Materials: All solvents were degassed, dried, and purified with the solvent purification system SPS-800 by MBraun and stored over activated 4 Å molecular sieves. All reactions were carried out under a nitrogen or argon atmosphere using standard Schlenk techniques and anhydrous, degassed solvents, unless otherwise stated. Quinazolin-4-amines **Qa**–**d** and **DMQa**–**d** were prepared as described previously.[14] *closo*-1,7-Dicarbadodecaborane(12)-1-acid chloride (**CbCOCl**)[16] and *closo*-9-Br-1,7-dicarbadodecaborane[17] were prepared according to the literature. Adamantane-1-carbonyl chloride (**AdmCOCl**) was prepared by refluxing the appropriate acid in thionyl chloride for 20 h and used without further purification. Benzyl chloride (**PhCOCl**) and all other starting materials and reagents are commercially available and were used as purchased. The NMR spectra were recorded on a BRUKER Avance III HD 400 MHz NMR spectrometer at 25 °C (^{1}H 400.13 MHz, ^{11}B 128.38 MHz, ^{13}C 100.63 MHz, two-dimensional (^{1}H–^{1}H COSY, ^{1}H–^{13}C HSQC, ^{1}H–^{13}C HMBC)). The chemical shifts δ are reported in parts per million (ppm). Tetramethylsilane (TMS) or solvent residual peaks were used as the internal reference in ^{1}H- and ^{13}C-NMR spectra, all other nuclei spectra were referenced to TMS using the Ξ scale.[30] The numbering scheme for ^{1}H- and ^{13}C-NMR signals is presented for each compound in the SI. Electrospray ionization mass spectrometry (ESI-MS) was carried out with an ESI-qTOF Impact II by Bruker Daltonics GmbH in positive mode. IR spectra were obtained with an FT-IR spectrometer Nicolet iS5 (ATR, transmission, Thermo Scientific) scanning between 4000–400 cm^{-1} with a KBr beam splitter (only selected frequencies given without assignment). Elemental analyses (C, H, and N) were performed with a Heraeus VARIO EL micro-analyzer. The melting points were determined in glass capillaries using a Gallenkamp apparatus and are uncorrected. Column chromatography was performed using a Biotage Isolera ONE and KP-SIL columns.

General procedure for preparation of *N*-carboranoyl 2-phenyl-quinazolin-4-amines: In a Schlenk flask, quinazoline (1.00 mmol) and NEt_3 (1.50–10.0 mmol) were dissolved in dry THF (3 mL/mmol). In a separate Schlenk flask, 1.00 eq. of *closo*-1,7-dicarbadodecaborane(12)-1-carbonyl chloride was dissolved in THF (2 mL/mmol) and added dropwise to the reaction. The reaction

mixture was then stirred at room temperature or under heating for 2–17 h. After removal of excess solvent under reduced pressure, water was added and the mixture was extracted with CH_2Cl_2. The combined organic phases were dried over $MgSO_4$ and concentrated. The crude product was purified by column chromatography on silica gel ($CHCl_3$ or *n*-hexane/EtOAc).

***N*-(*closo*-1,7-Dicarbadodecaboran(12)-1-oyl)-2-phenylquinazolin-4-amine (QCe)** was obtained from 2-phenylquinazolin-4-amine (1.00 eq.), NEt_3 (1.50 eq.) and carboranyl acid chloride (1.00 eq.) after 10 h colorless solid in 52% yield (102 mg) according to the general procedure described above. R_f = 0.49 (*n*-hexane/EtOAc, 6:1, *v/v*). **Mp.** = 240–242 °C ($CHCl_3$). **^{1}H-NMR** (400 MHz, $CDCl_3$): δ [ppm] = 15.03 (s, 1H, N**H**CO), 8.64 (d, $^3J_{HH}$ = 8.1 Hz, 1H, **H**5), 8.21–8.16 (m, 2H, **H**1′), 7.97–7.90 (m, 2H, **H**6, **H**8), 7.66–7.54 (m, 4H, **H**7, **H**2′, **H**3′), 4.03–1.40 (br, 10H, cluster-B**H**), 3.05 (s, 1H, cluster-C**H**). **^{13}C{^{1}H}-NMR** (101 MHz, $CDCl_3$): δ [ppm] = 159.3 (1 C, NH**C**O), 149.7 (1 C, C_q), 148.6 (1 C, C_q), 136.2 (1 C, **C**8), 132.3 (1 C, **C**7), 131.5 (1 C, C_{arom}), 129.4 (2 C, **C**5, **C**1′), 128.2 (1 C, **C**6), 128.1 (1 C, C_{arom}), 126.9 (2 C, **C**2′), 126.8 (1 C, C_{arom}), 119.5 (1 C, C_{arom}), 54.5 (1 C, cluster-**C**). **^{11}B{^{1}H}-NMR** (128 MHz, $CDCl_3$): δ [ppm] = −4.7 (s, 1B, **B**H), −7.7 (s, 1B, **B**H), −11.0 (s, 4B, **B**H), −13.5 (s, 2B, **B**H), −15.4 (s, 2B, **B**H). **HR-MS** (ESI(+), acetonitrile): *m/z* calc $[C_{17}H_{21}B_{10}N_3O]$ ($[M+H]^+$): 392.2761, found: 392.2780. **IR** (KBr): $\tilde{\nu}$ [cm^{-1}] = 3037, 2577, 1612, 1577, 1296, 743. **Elemental Analysis** ($C_{17}H_{21}B_{10}N_3O$) calc. (%): C 52.16, H 5.41, N 10.73 found (%): C 52.24, H 5.48, N 10.63.

***N*-(*closo*-1,7-Dicarbadodecaboran(12)-1-oyl)-2-(4-methoxyphenyl)-quinazolin-4-amine (QCf)** was obtained from 2-(4-methoxyphenyl)quinazolin-4-amine (1.00 eq.), NEt_3 (1.50 eq.) and carboranyl acid chloride (1.00 eq.) after 5 h colorless solid in 54% yield (127 mg) according to the general procedure described above. R_f = 0.65 ($CHCl_3$). **Mp.** = 240–242 °C ($CHCl_3$). **^{1}H-NMR** (400 MHz, $CDCl_3$): δ [ppm] = 14.95 (s, 1H, N**H**CO), 8.60 (d, $^3J_{HH}$ = 7.4 Hz, 1H, **H**8), 8.13 (d, $^3J_{HH}$ = 7.8 Hz, 2H, **H**2′), 7.93–7.83 (m, 2H, **H**5, **H**6), 7.58 (t, $^3J_{HH}$ = 7.5 Hz, 1H, **H**7), 7.05 (d, $^3J_{HH}$ = 8.4 Hz, 2H, **H**3′), 3.90 (s, 3H, O**CH$_3$**), 3.62–1.39 (br, 10H, cluster-B**H**), 3.05 (s, 1H, cluster-C**H**). **^{13}C{^{1}H}-NMR** (101 MHz, $CDCl_3$): δ [ppm] = 175.0 (1 C, NH**C**O), 163.2 (1 C, C_q), 159.5 (1 C, C_q), 150.2 (1 C, C_q), 148.6 (1 C, C_q), 136.3 (1 C, **C**7), 128.9 (2 C, **C**2′), 128.1 (1 C, **C**5/**C**6/**C**8), 127.8 (1 C, **C**5/**C**6/**C**8), 127.0 (1 C, **C**5/**C**6/**C**8), 123.9 (1 C, C_q), 119.4 (1 C, **C**4a), 114.9 (2 C, **C**3′), 55.7 (1 C, OCH_3), 54.7 (1 C, cluster-**C**). **^{11}B{^{1}H}-NMR** (128 MHz, $CDCl_3$): δ [ppm] = −4.6 (s, 1B), −7.7 (s, 1B), −10.9 (s, 4B), −13.5 (s, 2B), −15.4 (s, 2B). **HR-MS** (ESI(+), acetonitrile): *m/z* calc. $[C_{18}H_{23}B_{10}N_3O_2]$ ($[M+H]^+$): 423.2835, found: 423.2851. **IR** (KBr): $\tilde{\nu}$ [cm^{-1}] = 3043, 2597, 1580, 1311, 1258, 768, 723.

***N*-(*closo*-1,7-Dicarbadodecaboran(12)-1-oyl)-2-(3,4-dimethoxyphenyl)quinazolin-4-amine (QCg)** was obtained from 2-(3,4-dimethoxyphenyl)quinazolin-4-amine (1.00 eq.), NEt_3 (1.50 eq.), and carboranyl acid chloride (1.00 eq.) after 2 h as a colorless solid in 35% yield (91 mg) according to the general procedure described above. R_f = 0.52 (*n*-hexane/EtOAc, 2:1, *v/v*). **Mp.** = 279-281 °C ($CHCl_3$). **^{1}H-NMR** (400 MHz, $CDCl_3$): δ [ppm] = 14.98 (s, 1H, N**H**CO), 8.66–8.55 (m, 1H, **H**8), 7.97–7.80 (m, 3H, **H**5, **H**6, **H**2′), 7.68–7.56 (m, 2H, **H**7, **H**6′), 7.01 (d, $^3J_{HH}$ = 8.3 Hz, 1H, **H**5′), 4.06 (s, 3H, O**CH$_3$**), 3.98 (s, 3H, O**CH$_3$**), 3.62–1.35 (br, 10H, cluster-B**H**), 3.05 (s, 1H, cluster-C**H**). **^{11}B{^{1}H}-NMR** (128 MHz, $CDCl_3$): δ [ppm] = −4.6 (s, 1B), −7.5 (s, 1B), −10.9 (s, 4B), −13.4 (s, 2B), −15.4 (s, 2B). **HR-MS** (ESI(+), acetonitrile): *m/z* calc. $[C_{19}H_{25}B_{10}N_3O_3]$ ($[M+H]^+$): 453.2941, found: 453.2986. **IR** (KBr): $\tilde{\nu}$ [cm^{-1}] = 3031, 2598, 1566, 1293, 1261, 772.

***N*-(*closo*-1,7-Dicarbadodecaboran(12)-1-oyl)-2-(3,4,5-trimethoxyphenyl)quinazolin-4-amine (QCh)** was obtained from 2-(3,4,5-trimethoxyphenyl)quinazolin-4-amine (1.00 eq.), NEt_3 (1.50 eq.) and carboranyl acid chloride (1.00 eq.) after 1.5 h light yellow solid in 46% yield (108 mg) according to the general procedure described above. R_f = 0.55 (*n*-hexane/EtOAc, 2:1, *v/v*). **Mp.** = 236–237 °C ($CHCl_3$). **^{1}H-NMR** (400 MHz, $CDCl_3$): δ [ppm] = 14.94 (s, 1H, N**H**CO), 8.61 (d, $^3J_{HH}$ = 8.0 Hz, 1H, **H**8), 7.96–7.86 (m, 2H, **H**6, **H**5), 7.60 (t, $^3J_{HH}$ = 7,7 Hz, 1H, **H**7), 7.36 (s, 2H, **H**2′), 4.02 (s, 6H, O**CH$_3$**), 3.94 (s, 3H, O**CH$_3$**), 3.71–1.39 (br, 10H, cluster-B**H**), 3.04 (s, 1H, cluster-C**H**). **^{13}C{^{1}H}-NMR** (101 MHz, $CDCl_3$): δ [ppm] = 174.9 (1 C, NH**C**O), 159.3 (1 C, C_q), 153.9 (2 C, **C**3′), 149.7 (1 C, C_q), 148.7 (1 C, C_q), 141.9 (1 C, C_q), 136.3 (1 C, **C**7), 128.2 (1 C, **C**8/**C**6/**C**5), 128.0 (1 C, **C**8/**C**6/**C**5), 126.9 (1 C, **C**8/**C**6/**C**5), 119.5 (1 C, **C**4a), 104.5 (2 C, **C**2′), 61.1 (1 C, OCH_3), 56.6 (2 C, OCH_3), 54.7 (1 C, cluster-**C**). **^{11}B{^{1}H}-NMR** (128 MHz, $CDCl_3$): δ [ppm] = −4.6 (s, 1B), −7.6 (s, 1B), −10.9 (s, 4B), −13.5 (s, 2B), −15.4 (s, 2B). **HR-MS** (ESI(+), acetonitrile): *m/z* calc. $[C_{20}H_{27}B_{10}N_3O_4]$ ($[M+H]^+$): 483.3047, found: 483.3056. **IR** (KBr): $\tilde{\nu}$ [cm^{-1}] = 3060, 2939, 2598, 1584, 1285, 1258, 766, 728.

***N*-(*closo*-1,7-Dicarbadodecaboran(12)-1-oyl)-6,7-dimethoxy-2-phenylquinazolin-4-amine (DMQCe)** was obtained from 6,7-dimethoxy-2-phenylquinazolin-4-amine (1.00 eq.), NEt_3 (10.0 eq.) and carboranyl acid chloride (1.00 eq.) after 5 h at 40 °C light yellow solid in 24% yield (80 mg) according to the general procedure described above. R_f = 0.42 (*n*-hexane/EtOAc, 3:1, *v/v*). **Mp.** = 291–293 °C (*n*-pentane). **^{1}H-NMR** (400 MHz, $CDCl_3$): δ [ppm] = 15.12 (s, 1H, N**H**CO), 8.17–8.11 (m, 2H, **H**2′), 7.89 (s, 1H, **H**8), 7.57 (q, $^3J_{HH}$ = 5.1, 4.4 Hz, 3H, **H**3′, **H**4′), 7.29 (s, 1H, **H**5), 4.09 (s, 3H, O**CH$_3$**), 4.09 (s, 3H, O**CH$_3$**), 3.56–1.38 (br, 10H, cluster-B**H**), 3.04 (s, 1H, cluster-C**H**). **^{13}C{^{1}H}-NMR** (101 MHz, $CDCl_3$): δ [ppm] = 174.2 (1 C, **C**O), 157.8 (1 C, C_q), 157.5 (1 C, C_q), 150.5 (1 C, C_q), 147.9 (1 C, C_q), 147.4 (1 C, C_q), 132.2 (1 C, **C**4′), 131.8 (1 C, C_q), 129.5 (2 C, **C**3′/ **C**2′), 126.9 (2 C, **C**2′/ **C**3′), 113.7 (1 C, **C**4a), 108.1 (1 C, **C**8), 104.8 (1 C, **C**5), 56.7 (1 C, OCH_3), 56.4 (1 C, OCH_3), 54.6 (1 C, cluster-**C**H). **^{11}B{^{1}H}-NMR** (128 MHz, $CDCl_3$): δ [ppm] = −4.6 (s, 1B), −7.8 (s, 1B), −11.0 (s, 4B), −13.6 (s, 2B), −15.4 (s, 2B). **HR-MS** (ESI(+), acetonitrile): *m/z* calc. $[C_{19}H_{25}B_{10}N_3O_3]$ ($[M+H]^+$): 452.2972, found: 452.2986. **IR** (KBr): $\tilde{\nu}$ [cm^{-1}] = 3058, 2594, 1606, 1582, 1267, 1232, 714.

***N*-(*closo*-1,7-Dicarbadodecaboran(12)-1-oyl)-6,7-dimethoxy-2-(4-methoxyphenyl)quinazolin-4-amine (DMQCf)** was obtained from 6,7-dimethoxy-2-(4-methoxyphenyl)quinazolin-4-amine (1.00 eq.), NEt_3 (1.50 eq.) and carboranyl acid chloride (1.00 eq.) after 5 h under reflux conditions light yellow solid in 27% yield (66 mg) according to the general procedure described above. R_f = 0.27 ($CHCl_3$). **Mp.** = 282-284 °C ($CHCl_3$). **^{1}H-NMR** (400 MHz, $CDCl_3$): δ [ppm] = 15.04 (s, 1H, N**H**CO), 8.10 (d, $^3J_{HH}$ = 8.1 Hz, 2H, **H**2′), 7.86 (s, 1H, **H**8), 7.24 (s, 1H, **H**5), 7.04 (d, $^3J_{HH}$ = 8.7 Hz, 2H, **H**3′), 4.08 (s, 6H, O**CH$_3$**), 3.90 (s, 3H, O**CH$_3$**), 3.60–1.39 (br, 10H, cluster-B**H**), 3.03 (s, 1H, cluster-C**H**). **^{13}C{^{1}H}-NMR** (101 MHz, $CDCl_3$): δ [ppm] = 174.1 (1 C, NH**C**O), 162.9 (1 C, C_q), 157.4 (1 C, C_q), 150.1 (1 C, C_q), 147.7 (1 C, C_q), 128.6 (2 C, **C**2′), 114.9 (2 C, **C**3′), 107.8 (1 C, **C**5/**C**8), 104.8 (1 C, **C**5/**C**8), 56.7 (1 C, OCH_3), 56.4 (1 C, OCH_3), 55.7 (1 C, OCH_3), 54.6 (1 C, cluster-**C**H). **^{11}B{^{1}H}-NMR** (128 MHz, $CDCl_3$): δ [ppm] = −4.7 (s, 1B), −7.8 (s, 1B), −11.0 (s, 4B), −13.6 (s, 2B), −15.4 (s, 2B). **HR-MS** (ESI(+), acetonitrile): *m/z* calc. $[C_{20}H_{27}B_{10}N_3O_4]$ ($[M+H]^+$): 483.3047, found: 483.3050. **IR** (KBr): $\tilde{\nu}$ [cm^{-1}] = 3055, 2939, 2593, 1582, 1320, 1263, 769, 725.

***N*-(*closo*-1,7-Dicarbadodecaboran(12)-1-oyl)-6,7-dimethoxy-2-(3,4-dimethoxyphenyl)-quinazolin-4-amine (DMQCg)** was obtained from 6,7-dimethoxy-2-(3,4-dimethoxyphenyl)quinazolin-4-amine (1.00 eq.), NEt_3 (1.50 eq.) and carboranyl acid chloride (1.00 eq.) after 2.5 h under reflux conditions as a colorless solid in 47% yield (122 mg) according to the general procedure described above. R_f = 0.29 (*n*-hexane/EtOAc, 2:1, *v/v*). **Mp.** = 294–296 °C ($CHCl_3$). **^{1}H-NMR** (400 MHz, $CDCl_3$): δ [ppm] = 15.03 (s, 1H, N**H**CO), 7.84 (s, 1H, **H**8), 7.80 (s, 1H, **H**5), 7.57 (d, $^3J_{HH}$ = 8.3 Hz, 1H, **H**6′), 7.25 (s, 1H, **H**2′), 6.97 (d, $^3J_{HH}$ = 8.4 Hz, 1H, **H**5′), 4.08 (s, 3H, O**CH$_3$**), 4.06 (s, 3H, O**CH$_3$**), 4.04 (s, 3H, O**CH$_3$**), 3.96 (s, 3H O**CH$_3$**), 3.68–1.43 (br, 10H, cluster-B**H**), 3.04 (s, 1H, cluster-C**H**). **^{13}C{^{1}H}-NMR** (101 MHz, $CDCl_3$): δ [ppm] = 174.1 (1 C, NH**C**O), 157.3 (1 C, C_q), 152.5 (1 C, C_q), 150.1 (1 C, C_q), 149.8 (1 C, C_q), 147.5 (1 C, C_q), 124.4 (1 C, C_q), 119.6 (1 C, C_{Ar}H), 113.3 (1 C,

C_q), 111.1 (1 C, $C_{Ar}H$), 109.9 (1 C, $C_{Ar}H$), 107.8 (1 C, $C_{Ar}H$), 104.8 (1 C, $C_{Ar}H$), 56.7 (1 C, OCH_3), 56.4 (1 C, OCH_3), 56.3 (1 C, OCH_3), 56.2 (1 C, OCH_3), 54.6 (1 C, cluster-**C**H). **$^{11}B\{^1H\}$-NMR** (128 MHz, $CDCl_3$): δ [ppm] = −4.6 (s, 1B), −7.8 (s, 1B), −10.9 (s, 4B), −13.6 (s, 2B), −15.4 (s, 2B). **HR-MS** (ESI(+), acetonitrile): *m/z* calc. $[C_{21}H_{29}B_{10}N_3O_5]$ ($[M+H]^+$): 512.3183, found: 512.3197. **IR** (KBr): $\tilde{\nu}$ [cm^{-1}] = 3046, 2933, 2603, 1588, 1310, 1243, 767, 731.

General procedure for preparation of *N*-benzoyl and *N*-(adamant-1-oyl)-2-phenylquinazolin-4-amines: Under nitrogen atmosphere, quinazoline (1.00 mmol) and NEt_3 (1.50–10.0 mmol) were dissolved in dry THF (3 mL/mmol), and the appropriate acid chloride (1.00 eq.) was added dropwise/portionwise to the reaction. The mixture was stirred under reflux for 5 h. Excess solvent was removed under reduced pressure, water was added and the mixture was extracted with EtOAc. The combined organic phases were dried over $MgSO_4$ and concentrated. The crude product was purified by column chromatography on silica gel (*n*-hexane/EtOAc).

***N*-Benzoyl-2-phenylquinazolin-4-amine (QPe)** was obtained from 2-phenylquinazolin-4-amine and benzoyl chloride as a light yellow solid in 52% yield (169 mg) according to the general procedure described above. R_f = 0.64 (*n*-hexane/EtOAc, 2:1, *v/v*). **Mp.** = 156–158 °C ($CHCl_3$). **^{1}H-NMR** (400 MHz, $CDCl_3$): δ [ppm] = 16.08 (s, 1H, N**H**CO), 8.81 (d, $^3J_{HH}$ = 8.1 Hz, 1H, **H**8), 8.50 (d, $^3J_{HH}$ = 7.5 Hz, 2H, **H**2′), 8.30–8.24 (m, 2H, **H**2″), 7.90 (d, $^3J_{HH}$ = 4.5 Hz, 2H, H_{Ar}), 7.64–7.49 (m, 7H, H_{Ar}, **H**7, **H**3′, **H**3″). **$^{13}C\{^1H\}$-NMR** (101 MHz, $CDCl_3$): δ [ppm] = 180.9 (1 C, NH**C**O), 159.3 (1 C, C_q), 149.6 (1 C, C_q), 149.4 (1 C, C_q), 137.7 (1 C, C_q), 135.5 (1 C, C_q), 132.5 (1 C, C_q), 132.4 (1 C, $C_{Ar}H$), 132.2 (1 C, $C_{Ar}H$), 130.0 (2 C, **C**2′), 129.5 (1 C, $C_{Ar}H$), 128.4 (1 C, $C_{Ar}H$), 127.7 (1 C, $C_{Ar}H$), 127.2 (2 C, **C**2″), 126.5 (1 C, **C**8), 120.3 (1 C, $C_{Ar}H$). **HR-MS** (ESI(+), acetonitrile): *m/z* calc. $[C_{21}H_{15}N_3O]$ ($[M+H]^+$): 326.1279, found: 326.1278. **IR** (KBr): $\tilde{\nu}$ [cm^{-1}] = 3046, 2933, 2603, 1588, 1310, 1243, 767, 731. **Elemental Analysis** ($C_{21}H_{15}N_3O$) calc. (%): C 77.52, H 4.65 N 12.91, found (%): C 77.66, H 4.71, N 12.82.

***N*-(Adamant-1-oyl)-2-phenylquinazolin-4-amine (QAe)** was obtained from 2-phenylquinazolin-4-amine and adamantane-1-carbonyl chloride as an off-white solid in 57% yield (218 mg) according to the general procedure described above. R_f = 0.83 (*n*-hexane/EtOAc, 2:1, *v/v*). **Mp.** = 157–159 °C ($CHCl_3$). **^{1}H-NMR** (400 MHz, DMSO): δ [ppm] 10.30 (s, 1H, N**H**CO), 8.56–8.51 (m, 2H, **H**2′), 8.04 (dd, $^3J_{HH}$ = 8.5, 1.2 Hz, 1H, **H**8), 7.98 (ddd, $^3J_{HH}$ = 8.4, 6.7, 1.4 Hz, 1H, **H**7), 7.90 (dd, $^3J_{HH}$ = 8.4, 1.4 Hz, 1H, **H**5), 7.66 (ddd, $^3J_{HH}$ = 8.2, 6.8, 1.3 Hz, 1H, **H**6), 7.57 (dd, $^3J_{HH}$ = 5.3, 2.0 Hz, 3H, **H**3′, **H**4′), 2.50 (p, $^3J_{HH}$ = 1.8 Hz, 4H, Adm-**H**), 2.08 (s, 7H, Adm-**H**), 1.76 (s, 4H, Adm-**H**). **$^{13}C\{^1H\}$-NMR** (101 MHz, $CDCl_3$): δ [ppm] = 177.3 (1 C, NH**C**O), 159.4 (1 C, C_q), 159.2 (1 C, C_q), 151.7 (1 C, C_q), 137.2 (1 C, **C**1′), 134.4 (1 C, **C**7), 130.8 (1 C, **C**4′), 128.6 (2 C, **C**3′), 128.1 (3 C, **C**8, **C**2′), 126.9 (1 C, **C**6), 126.0 (1 C, **C**5), 118.4 (1 C, **C**4a), 41.4 (1 C, Adm-C_q), 38.1 (3 C, Adm-**C**), 36.0 (3 C, Adm-**C**), 27.7 (3 C, Adm-**C**). **IR** (KBr): $\tilde{\nu}$ [cm^{-1}] = 3288, 2902, 2850, 1672, 1619, 1552, 1482, 1390, 1352, 1226, 1108, 1027, 770, 759. **HR-MS** (ESI(+), acetonitrile): *m/z* calc $[C_{25}H_{25}N_3O]$ ($[M+H]^+$): 384.2076, found: 384.2069. **Elemental Analysis** ($C_{25}H_{26}N_3O$) calc. (%): C 78.30, H 6.57 N 10.96, found (%): C 78.19, H 6.55, N 10.86.

General procedure for preparation of *N*-phenyl 2-phenylquinazolin-4-amines: A Schlenk flask was charged with a quinazolin-4-amine (1.00 mmol), CuI (10 mol%) and potassium carbonate (1.00 mmol). The flask was evacuated three times and backfilled with argon. DMF (4 mL) and iodobenzene (124 μL, 1.10 mmol) were added and the mixture was heated to 130 °C overnight. After cooling to room temperature, water (10 mL) and conc. NH_4OH (0.5 mL) were added and the mixture was extracted with EtOAc (3×50 mL). After removal of solvents and volatiles, the crude product was purified by column chromatography on silica gel (*n*-hexane/EtOAc).

***N*-Phenyl-2-(3,4-dimethoxyphenyl)-quinazolin-4-amine (QPc)** was obtained from 2-(3,4-dimethoxyphenyl)quinazolin-4-amine as a light yellow solid in 91% yield (324 mg) according to the general procedure described above. R_f = 0.72 (*n*-hexane/EtOAc, 1:1, *v/v*). **^{1}H-NMR** (400 MHz, $CDCl_3$): δ [ppm] = 8.18 (dd, $^3J_{HH}$ = 4.4, 2.5 Hz, 2H, **H**2′, **H**6′), 7.96 (dd, $^3J_{HH}$ = 8.4, 1.2 Hz, 1H, **H**8), 7.92–7.88 (m, 2H, **H**2″), 7.86 (dd, $^3J_{HH}$ = 8.4, 1.2 Hz, 1H, **H**5), 7.77 (ddd, $^3J_{HH}$ = 8.4, 6.9, 1.3 Hz, 1H, **H**7), 7.50 (d, $^3J_{HH}$ = 4.1 Hz, 1H, **H**4′), 7.48–7.41 (m, 3H, **H**6, **H**3″), 7.18 (t, $^3J_{HH}$ = 7.4 Hz, 1H, **H**4″), 6.99 (d, $^3J_{HH}$ = 8.9 Hz, 1H, **H**5′), 4.02 (s, 3H, OCH_3), 3.95 (s, 3H, OCH_3). **$^{13}C\{^1H\}$-NMR** (101 MHz, $CDCl_3$): δ [ppm] = 160.1 (1 C, C_q), 157.2 (1 C, C_q), 151.3 (1 C, C_q), 151.1 (1 C, C_q), 148.8 (1 C, C_q), 138.8 (1 C, C_q), 132.9 (1 C, **C**7), 131.6 (1 C, $C_{Ar}H$), 129.2 (1 C, **C**8), 128.9 (2 C, **C**3″), 125.8 (1 C, **C**4′), 124.2 (1 C, **C**4″), 121.8 (1 C, **C**6′), 121.6 (2 C, **C**2″), 120.4 (1 C, **C**5), 113.8 (1 C, $C_{Ar}H$), 111.3 (1 C, **C**2′), 110.8 (1 C, **C**5′), 56.1 (1 C, OCH_3), 55.9 (1 C, OCH_3). **IR** (KBr): $\tilde{\nu}$ [cm^{-1}] = 3000, 2957, 2836, 2361, 1616, 1601, 1526, 1405, 1367, 1125, 1021, 754. **HR-MS** (ESI(+), acetonitrile): *m/z* calc. $[C_{22}H_{19}N_3O_2]$ ($[M+H]^+$): 358.1550, found: 358.1554. **Elemental Analysis** ($C_{22}H_{19}N_3O_2$) calc. (%): C 73.93, H 5.36, N 11.76 found (%): C 73.98, H 5.41, N 11.73.

***N*-Phenyl-6,7-dimethoxy-2-phenylquinazolin-4-amine (DMQPa)** was obtained from 6,7-dimethoxy-2-phenylquinazolin-4-amine as an off-white solid in 52% yield (184 mg) according to the general procedure described above. R_f = 0.51 (*n*-hexane/EtOAc, 3:2, *v/v*). **^{1}H-NMR** (400 MHz, $CDCl_3$): δ [ppm] = 8.50 (dd, $^3J_{HH}$ = 8.0, 1.7 Hz, 2H, **H**2′), 7.87–7.83 (m, 2H, **H**2″), 7.51–7.43 (m, 5H, **H**3′, **H**3″, **H**4′), 7.35 (s, 1H, **H**8), 7.21–7.15 (m, 2H, **H**4″, N**H**), 7.02 (s, 1H, **H**5), 4.04 (s, 3H, OCH_3), 4.01 (s, 3H, OCH_3). **$^{13}C\{^1H\}$-NMR** (101 MHz, $CDCl_3$): δ [ppm] = 159.4 (1 C, C_q), 156.3 (1 C, C_q), 154.9 (1 C, C_q), 149.4 (1 C, C_q), 148.7 (1 C, C_q), 139.2 (1 C, C_q), 138.9 (1 C, C_q), 130.1 (1 C, **C**4′), 129.1 (2 C, **C**3′/**C**3″), 128.51 (2 C, **C**3′/**C**3″), 128.3 (2 C, **C**2′), 123.9 (1 C, **C**4″), 121.5 (2 C, **C**2″), 108.6 (1 C, **C**8), 107.8 (1 C, C_q), 99.4 (1 C, **C**5), 56.4 (2 C, OCH_3). **HR-MS** (ESI(+), acetonitrile): *m/z* calc. $[C_{22}H_{19}N_3O_2]$ ($[M+H]^+$): 358.1550, found: 358.1578. **Elemental Analysis** ($C_{22}H_{19}N_3O_2$) calc. (%): C 73.93, H 5.36, N 11.76 found (%): C 73.89, H 5.40, N 11.80.

***N*-Phenyl-6,7-dimethoxy-2-(4-methoxyphenyl)quinazolin-4-amine (DMQPb)** was obtained from 6,7-dimethoxy-2-(4-methoxyphenyl)quinazolin-4-amine as a beige solid in 44% yield (198 mg) according to the general procedure described above. R_f = 0.49 (*n*-hexane/EtOAc, 3:2, *v/v*). **Mp.** = 214–216 °C (pentane). **^{1}H-NMR** (400 MHz, $CDCl_3$): δ [ppm] = 8.45 (d, $^3J_{HH}$ = 8.9 Hz, 2H, **H**2′), 7.83 (d, $^3J_{HH}$ = 7.8 Hz, 2H, **H**2″), 7.45 (dd, $^3J_{HH}$ = 8.5, 7.4 Hz, 2H, **H**3″), 7.32 (s, 1H, **H**8), 7.20–7.14 (m, 2H, **H**4″, N**H**), 7.00 (d, $^3J_{HH}$ = 8.5 Hz, 3H, **H**5, **H**3′), 4.04 (s, 3H, OCH_3), 4.01 (s, 3H, OCH_3), 3.88 (s, 3H, OCH_3). **$^{13}C\{^1H\}$-NMR** (101 MHz, $CDCl_3$): δ [ppm] = 161.4 (1 C, C_q), 159.2 (1 C, C_q), 156.2 (1 C, C_q), 154.8 (1 C, C_q), 149.0 (1 C, C_q), 148.7 (1 C, C_q), 139.2 (1 C, C_q), 131.6 (1 C, C_q), 129.8 (2 C, **C**2′), 129.1 (2 C, **C**3″), 123.8 (1 C, **C**4″), 121.5 (2 C, **C**2″), 113.8 (2 C, **C**3′), 108.4 (1 C, **C**8), 107.5 (1 C, **C**4a), 99.5 (1 C, **C**5), 56.4 (2 C, OCH_3), 55.5 (1 C, OCH_3). **HR-MS** (ESI(+), acetonitrile): *m/z* calc. $[C_{23}H_{21}N_3O_3]$ ($[M+H]^+$): 388.1655, found: 388.1650. **IR** (KBr): $\tilde{\nu}$ [cm^{-1}] = 3362, 2964, 2835, 1599, 1411, 1358, 1222, 1028, 999, 847. **Elemental Analysis** ($C_{23}H_{21}N_3O_3$) calc. (%): C 71.30, H 5.46, N 10.85 found (%): C 71.33, H 5.50, N 10.79.

***N*-Phenyl-6,7-dimethoxy-2-(3,4-dimethoxyphenyl)quinazolin-4-amine (DMQPc)** was obtained from 6,7-dimethoxy-2-(3,4-dimethoxyphenyl)quinazolin-4-amine as an off-white solid in 51% yield (213 mg) according to the general procedure described above. R_f = 0.41 (*n*-hexane/EtOAc, 1:1, *v/v*). **Mp.** = 210-213 °C (pentane). **^{1}H-NMR** (400 MHz, $CDCl_3$): δ [ppm] = 8.12 (d, $^3J_{HH}$ = 7.7 Hz, 2H, **H**2′, **H**6′), 7.84 (d, $^3J_{HH}$ = 7.6 Hz, 2H, **H**2″), 7.42 (t, $^3J_{HH}$ = 7.7 Hz, 2H, **H**3″), 7.26 (s, 1H, **H**8), 7.16 (t, $^3J_{HH}$ = 7.4 Hz, 1H, **H**4″), 7.05 (s, 1H, **H**5), 6.97 (d, $^3J_{HH}$ = 8.3 Hz, 1H, **H**5′), 4.03 (s, 3H, OCH_3), 4.01 (s, 3H, OCH_3), 4.00 (s, 3H, OCH_3), 3.95 (s, 3H, OCH_3). **$^{13}C\{^1H\}$-NMR** (101 MHz, $CDCl_3$): δ [ppm] = 158.9 (1 C, C_q), 158.2 (1 C, C_q), 156.2 (1 C, C_q), 154.9 (1 C, C_q), 150.9

(1 C, C_q), 149.1 (1 C, C_q), 148.8 (1 C, C_q), 139.2 (1 C, C_q), 131.8 (1 C, C_q), 128.9 (2 C, C3''), 124.0 (1 C, C5), 121.7 (2 C, C2''), 121.3 (1 C, C_q), 111.1 (1 C, C6'), 110.9 (1 C, C2'), 108.3 (1 C, C8), 107.5 (1 C, C_q), 99.6 (1 C, C5'), 56.4 (2 C, OCH_3), 56.1 (1 C, OCH_3), 55.9 (1 C, OCH_3). **HR-MS** (ESI(+), acetonitrile): *m/z* calc. $[C_{24}H_{23}N_3O_4]$ ($[M+H]^+$): 418.1761, found: 418.1771. **IR** (KBr): $\tilde{\nu}$ [cm^{-1}] = 3353, 2991, 2932, 2836, 1600, 1569, 1511, 1417, 1216, 1026, 849. **Elemental Analysis** ($C_{24}H_{23}N_3O_4$) calc. (%): C 69.05, H 5.55, N 10.07 found (%): 68.98, H 5.63, N 10.01.

***N*-Phenyl-6,7-dimethoxy-2-(3,4,5-trimethoxyphenyl)quinazolin-4-amine (DMQPd)** was obtained from 6,7-dimethoxy-2-(3,4,5-trimethoxy-phenyl)quinazolin-4-amine as a light yellow solid in 74% yield (331 mg) according to the general procedure described above. R_f = 0.34 (*n*-hexane/EtOAc, 2:1, *v/v*). **Mp.** = 224–226 °C (*n*-pentane). **^{1}H-NMR** (400 MHz, $CDCl_3$): δ [ppm] = 7.88–7.83 (m, 4H, H2', H2''), 7.41 (t, $^3J_{HH}$ = 7.8 Hz, 2H, H3''), 7.36 (s, 1H, H8), 7.25 (s, 1H, NH), 7.16 (t, $^3J_{HH}$ = 7.4 Hz, 1H, H4''), 7.05 (s, 1H, H5), 4.05 (s, 3H, OCH_3), 4.02 (s, 3H, OCH_3), 3.99 (s, 6H, OCH_3), 3.92 (s, 3H, OCH_3). **^{13}C{^{1}H}-NMR** (101 MHz, $CDCl_3$): δ [ppm] = 158.6 (1 C, C_q), 156.2 (1 C, C_q), 154.9 (1 C, C_q), 153.2 (1 C, C_q), 149.3 (1 C, C_q), 139.9 (1 C, C_q), 139.2 (1 C, C_q), 134.3 (1 C, C_q), 128.8 (2 C, C3''), 124.1 (1 C, C4''), 121.9 (2 C, C2''), 108.4 (1 C, C8), 107.6 (1 C, C_q), 105.2 (2 C, C2'), 99.5 (1 C, C5), 61.1 (1 C, OCH_3), 56.4 (1 C, OCH_3), 56.4 (2 C, OCH_3), 56.1 (2 C, OCH_3). **HR-MS** (ESI(+), acetonitrile): *m/z* calc. $[C_{25}H_{25}N_3O_5]$ ($[M+H]^+$): 448.1867, found: 448.1859. **IR** (KBr): $\tilde{\nu}$ [cm^{-1}] = 3556, 3350, 2993, 2932, 2835, 1625, 1600, 1568, 1506, 1409, 1334, 1222, 1121, 1033, 864. **Elemental Analysis** ($C_{25}H_{25}N_3O_5$) calc. (%): C 67.10, H 5.63, N 9.39 found (%): 67.18, H 5.70, N 9.34.

General procedure for preparation of 4-chloro-2-phenylquinazolines: In a 100 mL round-bottom flask, 2-aminobenzamide (1.00 eq.) and benzaldehyde (1.05 eq.) were dissolved in EtOH (10 mL/mmol). Iodine (1.10 eq.) was added to the stirred solution and the reaction mixture was heated to reflux overnight. After cooling to room temperature, 5% aq. $Na_2S_2O_3$ solution was added and the mixture was extracted with EtOAc (3×50 mL). The combined organic layers were dried over $MgSO_4$, solvents were removed under reduced pressure and the crude product was washed with hot *n*-hexane. The solid residue was placed in an ice bath and $POCl_3$ (1 mL/10 mg crude) was added slowly under stirring. The mixture was allowed to warm to rt and heated to 120 °C overnight. The mixture was then cooled to rt and residual $POCl_3$ was removed under reduced pressure. Iced water was added and the pH was adjusted to 7 with aq. $NaHCO_3$ solution. The mixture was extracted with CH_2Cl_2, and the combined organic phases were dried over $MgSO_4$. The obtained solids were used without further purification.

General procedure for preparation of *N*-adamantyl-2-phenylquinazolines: Dioxane (3 mL) was added to a mixture of 4-chloroquinazoline (0.50 mmol), Cs_2CO_3 (1.25 mmol) and adamantyl amine (1.00 mmol) under argon; for compounds **DMQAb** and **DMQAc**, DMF (3 mL) was used. The mixture was heated to 110 °C for 24 h. After cooling to room temperature, water (10 mL) was added and the mixture was extracted with EtOAc (3×30 mL). The combined EtOAc extracts were concentrated under reduced pressure and the crude product was purified by column chromatography on silica gel (*n*-hexane/EtOAc).

***N*-(1-Adamantyl)-2-(3,4-dimethoxyphenyl)-quinazolin-4-amine (QAc)** was obtained from 4-chloro-2-(3,4-dimethoxyphenyl)quinazoline as a light yellow solid in 70% yield (145 mg) according to the general procedure described above. R_f = 0.29 (*n*-hexane/EtOAc, 7:3, *v/v*). **Mp.** = 169–171 °C (*n*-pentane). **^{1}H-NMR** (400 MHz, $CDCl_3$): δ [ppm] = 8.22–8.17 (m, 2H, H2', H6'), 7.86 (d, $^3J_{HH}$ = 8.3 Hz, 1H, H8), 7.72–7.67 (m, 1H, H7), 7.62 (d, $^3J_{HH}$ = 8.2 Hz, H5), 7.40–7.35 (m, 1H, H6), 7.00 (d, $^3J_{HH}$ = 8.1 Hz, 1H, H5'), 5.43 (s, 1H, NH), 4.05 (s, 3H, OCH_3), 3.97 (s, 3H, OCH_3), 2.40 (d, $^3J_{HH}$ = 2.9 Hz, 6H, Adm-H), 2.22 (q, $^3J_{HH}$ = 3.3 Hz, 3H, Adm-H), 1.81 (d, $^3J_{HH}$ = 3.2 Hz, 6H, Adm-H). **^{13}C{^{1}H}-NMR** (101 MHz, $CDCl_3$): δ [ppm] = 159.8 (1 C, C_q), 158.9 (1 C, C_q), 150.9 (1 C, C_q), 148.8 (1 C, C_q), 133.2 (1 C, C_q), 132.4 (1 C, C_q), 132.3 (1 C, C7), 129.1 (1 C, C8), 125.0 (1 C, C6), 121.7 (1 C, C6'), 120.5 (1 C, C5), 116.6 (1 C, C_q), 114.0 (1 C, C_q), 111.2 (1 C, C2'), 110.8 (1 C, C5'), 56.1 (1 C, OCH_3), 56.0 (1 C, OCH_3), 53.3 (1 C, Adm-C), 41.9 (3 C, Adm-C), 36.8 (3 C, Adm-C), 29.8 (3 C, Adm-C). **HR-MS** (ESI(+), acetonitrile): *m/z* calc. $[C_{26}H_{29}N_3O_2]$ ($[M+H]^+$): 416.2333, found: 416.2337. **IR** (KBr): $\tilde{\nu}$ [cm^{-1}] = 3438, 3346, 2900, 2845, 1568, 1514, 1417, 1355, 1262, 1223, 1112, 1029, 761. **Elemental Analysis** ($C_{26}H_{29}N_3O_2$) calc. (%): C 75.15, H 7.03, N 10.11 found (%): C 75.19, H 7.12, N 10.02.

***N*-(1-Adamantyl)-6,7-dimethoxy-2-phenylquinazolin-4-amine (DMQAa)** was obtained from 6,7-dimethoxy-2-phenylquinazolin-4-amine as an off-white solid in 67% yield (140 mg) according to the general procedure described above. R_f = 0.49 (*n*-hexane/EtOAc, 2:1, *v/v*). **Mp.** = 146–148 °C (*n*-pentane). **^{1}H-NMR** (400 MHz, $CDCl_3$): δ [ppm] = 8.53–8.49 (m, 2H, H2'), 7.51–7.40 (m, 3H, H3', H4'), 7.25 (s, 1H, H8), 6.80 (s, 1H, H5), 5.10 (s, 1H, NH), 4.00 (s, 3H, OCH_3), 3.98 (s, 3H, OCH_3), 2.38 (d, $^3J_{HH}$ = 2.9 Hz, 6H, Adm-H), 2.23–2.18 (m, 3H, Adm-H), 1.80 (p, $^3J_{HH}$ = 2.7 Hz, 6H, Adm-H). **^{13}C{^{1}H}-NMR** (101 MHz, $CDCl_3$): δ [ppm] = 158.8 (1 C, C_q), 157.8 (1 C, C_q), 153.9 (1 C, C7), 148.4 (1 C, C6), 147.5 (1 C, C8a), 139.3 (1 C, C1'), 129.5 (1 C, C4'), 128.2 (2 C, C3'), 127.9 (2 C, C2'), 108.3 (1 C, C8), 107.5 (1 C, C4a), 99.5 (1 C, C5), 56.2 (1 C, OCH_3), 56.1 (1 C, OCH_3), 53.1 (1 C, Adm-C), 41.7 (3 C, Adm-C), 36.6 (3 C, Adm-C), 29.6 (3 C, Adm-C). **HR-MS** (ESI(+), acetonitrile): *m/z* calc. $[C_{26}H_{29}N_3O_2]$ ($[M+H]^+$): 416.2333, found: 416.2364. **IR** (KBr): $\tilde{\nu}$ [cm^{-1}] = 3418, 3058, 3005, 2838, 1602, 1572, 1523, 1440, 1349, 1236, 1178, 1021, 942, 834. **Elemental Analysis** ($C_{26}H_{29}N_3O_2$) calc. (%): C 75.15, H 7.03, N 10.11 found (%): C 75.28, H 7.09, N 10.01.

***N*-(1-Adamantyl)-6,7-dimethoxy-2-(4-methoxyphenyl)quinazolin-4-amine (DMQAb)** was obtained from 6,7-dimethoxy-2-(4-methoxyphenyl)quinazolin-4-amine as a beige solid in 83% yield (186 mg) according to the general procedure described above. R_f = 0.36 (*n*-hexane/EtOAc, 1:1, *v/v*). **Mp.** = 197–199 °C ($CHCl_3$). **^{1}H-NMR** (400 MHz, $CDCl_3$): δ [ppm] = 8.50–8.43 (m, 2H, H2'), 7.24 (s, 1H, H8), 7.04–6.97 (m, 2H, H3'), 6.79 (s, 1H, H5), 5.06 (s, 1H, NH), 4.01 (d, $^3J_{HH}$ = 7.7 Hz, 6H, OCH_3), 3.88 (s, 3H, OCH_3), 2.39 (d, $^3J_{HH}$ = 2.9 Hz, 6H, Adm-H), 2.25–2.19 (m, 3H, Adm-H), 1.81 (p, $^3J_{HH}$ = 2.9 Hz, 6H, Adm-H). **^{13}C{^{1}H}-NMR** (101 MHz, $CDCl_3$): δ [ppm] = 161.2 (1 C, C4), 158.9 (1 C, C_q), 157.9 (1 C, C_q), 154.1 (1 C, C6), 148.3 (1 C, C8a), 129.7 (2 C, C2'), 113.8 (2 C, C3'), 108.4 (1 C, C8), 107.4 (1 C, C4a), 99.8 (1 C, C5), 56.4 (2 C, OCH_3), 56.3 (2 C, OCH_3), 55.5 (2 C, OCH_3), 53.2 (1 C, Adm-C), 41.9 (3 C, Adm-C), 36.9 (3 C, Adm-C), 29.9 (3 C, Adm-C). **HR-MS** (ESI(+), acetonitrile): *m/z* calc. $[C_{27}H_{31}N_3O_3]$ ($[M+H]^+$): 446.2444, found: 446.2441. **IR** (KBr): $\tilde{\nu}$ [cm^{-1}] = 2902, 2846, 1606, 1584, 1515, 1495, 1427, 1356, 1243, 1210, 1160, 1031, 1003, 841, 791. **Elemental Analysis** ($C_{27}H_{31}N_3O_3$) calc. (%): C 72.78, H 7.01, N 9.43 found (%): C 72.89, H 7.12, N 9.30.

***N*-(1-Adamantyl)-6,7-dimethoxy-2-(3,4-dimethoxyphenyl)quinazolin-4-amine (DMQAc)** was obtained from 6,7-dimethoxy-2-(3,4-dimethoxyphenyl)quinazolin-4-amine as an off-white solid in 79% yield (187 mg) according to the general procedure described above. R_f = 0.27 (*n*-hexane/EtOAc, 1:1, *v/v*). **Mp.** = 246–248 °C ($CHCl_3$). **^{1}H-NMR** (400 MHz, $CDCl_3$): δ [ppm] = 8.14 (d, $^3J_{HH}$ = 7.1 Hz, 2H, H2', H6'), 7.26 (s, 1H, H8), 6.99 (d, $^3J_{HH}$ = 9.0 Hz, 1H, H3'), 6.81 (s, 1H, H5), 5.09 (s, 1H, NH), 4.03 (s, 3H, OCH_3), 4.02 (s, 3H, OCH_3), 4.00 (s, 3H, OCH_3), 3.95 (s, 3H, OCH_3), 2.40 (d, $^3J_{HH}$ = 2.9 Hz, 6H, Adm-H), 2.23–2.17 (m, 3H, Adm-H), 1.81 (d, $^3J_{HH}$ = 3.5 Hz, 6H, Adm-H). **^{13}C{^{1}H}-NMR** (101 MHz, $CDCl_3$): δ [ppm] = 157.9 (1 C, C4), 154.2 (1 C, C2), 150.7 (1 C, C7), 148.8 (1 C, C6), 148.4 (1 C, C8a), 121.3 (1 C, C6'), 110.9 (1 C, C2'), 110.8 (1 C, C5'), 108.4 (1 C, C8), 107.4 (1 C, C4a), 99.9 (1 C, C5), 56.4 (1 C, OCH_3), 56.3 (1 C, OCH_3), 56.1 (1 C, OCH_3), 55.9 (1 C, OCH_3), 53.2 (1 C, Adm-C), 42.0 (3 C, Adm-C), 36.9 (3 C, Adm-C), 29.9 (3 C, Adm-C). **HR-MS** (ESI(+), acetonitrile):

m/z calc. $[C_{28}H_{33}N_3O_4]$ ($[M+H]^+$): 476.2549, found: 476.2544. **IR** (KBr): $\tilde{\nu}$ [cm^{-1}] = 2904, 2847, 1621, 1572, 1513, 1498, 1425, 1356, 1307, 1266, 1223, 1070, 1025, 875. **Elemental Analysis** ($C_{28}H_{33}N_3O_4$) calc. (%): C 70.71, H 6.99, N 8.84 found (%): C 70.63, H 7.07, N 8.77.

***N*-(1-Adamantyl)-6,7-dimethoxy-2-(3,4,5-trimethoxyphenyl)-quinazolin-4-amine (DMQAd)** was obtained from 6,7-dimethoxy-2-(3,4,5-trimethoxy-phenyl)quinazolin-4-amine as an off-white solid in 47% yield (119 mg) according to the general procedure described above. R_f = 0.24 (*n*-hexane/EtOAc, 1:1, *v/v*). **Mp.** = 208–211 °C (*n*-pentane). **^{1}H-NMR** (400 MHz, $CDCl_3$): δ [ppm] = 7.86 (s, 2H, **H**2′), 7.28 (s, 1H, **H**8), 6.80 (s, 1H, **H**5), 5.08 (s, 1H, N**H**), 4.03 (s, 3H, O**CH$_3$**), 4.01 (s, 9H, O**CH$_3$**), 3.92 (s, 3H, O**CH$_3$**), 2.41 (d, $^3J_{HH}$ = 2.9 Hz, 6H, Adm-**H**), 2.24–2.19 (m, 3H, Adm-**H**), 1.80 (d, $^3J_{HH}$ = 3.0 Hz, 6H, Adm-**H**). **^{13}C{^{1}H}-NMR** (101 MHz, $CDCl_3$): δ [ppm] = 158.5 (1 C, **C$_q$**), 157.9 (1 C, **C$_q$**), 154.2 (1 C, **C**7), 153.2 (2 C, **C**3′), 148.6 (1 C, **C**6), 147.7 (1 C, **C**8a), 139.7 (1 C, **C**4′), 135.1 (1 C, **C**1′), 108.5 (1 C, **C**8), 107.6 (1 C, **C**4a), 105.2 (2 C, **C**2′), 99.8 (1 C, **C**5), 61.1 (1 C, O**CH$_3$**), 56.4 (1 C, O**CH$_3$**), 56.3 (1 C, O**CH$_3$**), 56.2 (2 C, O**CH$_3$**), 53.2 (1 C, Adm-**C**), 42.1 (3 C, Adm-**C**), 36.8 (3 C, Adm-**C**), 29.9 (3 C, Adm-**C**). **HR-MS** (ESI(+), acetonitrile): *m/z* calc. $[C_{29}H_{35}N_3O_5]$ ($[M+H]^+$): 506.2649, found: 506.2646. **IR** (KBr): $\tilde{\nu}$ [cm^{-1}] = 3396, 2903, 2846, 1620, 1566, 1497, 1423, 1408, 1246, 1122, 1071, 1002, 874, 850. **Elemental Analysis** ($C_{29}H_{35}N_3O_5$) calc. (%): C 68.89, H 6.98, N 8.31 found (%): C 68.95, H 7.05, N 8.29.

Biological Investigations

Cultivation of MDCKII cells: MDCKII-hABCG2 and MDCKII-WT cells were purchased from Alfred Schinkel (Het Nederlands Kanker Instituut, Amsterdam, Netherlands) and were cultivated in Minimum Essential Medium (MEM) with Earle's Salts (2.2 g/L $NaHCO_3$, stable glutamine; Biowest, Nuaillé, France) supplemented with 10% (*v/v*) fetal calf serum (Life Technology, Karlsruhe, Germany), 1% (*v/v*) non-essential amino acids (Biowest, Nuaillé, France), 100 U/mL penicillin and 100 μg/mL streptomycin (Biowest, Nuaillé, France). Cells were grown in humidified atmosphere (37 °C, 5% CO_2) and were sub-cultured every 3 to 4 days using 0.05% trypsin/0.02% ethylenediaminetetraacetic acid (EDTA; Biowest, Nuaillé, France) up to a total of 14 passages.

Determination of cell viability by WST-1 cell proliferation assay: MDCKII-hABCG2 cells and their parental MDCKII-WT cells were seeded in 96-well plates (TPP, Trasadingen, Switzerland) in a density of 2×10^4 cells/mL and 3×10^4 cells/mL, respectively. After 48 h, cells were incubated with increasing concentrations up to 50 μM of compounds (**QCe**, **QAe**, **QPe**, **DMQAc**, **DMQPc**, **DMQAd**, **DMQPd**), with 0.1% Triton X-100 as positive control and solvent (0.1% DMSO) as negative control for 48 h. Afterwards, the substance-specific cytotoxicity was determined by WST-1 assay as previously described.[20] Cell viability was determined by microplate reader at 450 nm (Tecan Sunrise, Crailsheim, Germany).

Determination of ABCG2 interaction with Hoechst 33342 accumulation assay: Hoechst 33342 accumulation assay was used to detect an interaction of the investigated compounds with the human ABCG2 transporter as described previously.[14] MDCKII-hABCG2 (2×10^4 cells/mL) and MDCKII-WT (3×10^4 cells/mL) cells were seeded in 96-well plates and cultured for 72 h. Afterwards, sub confluent monolayers were treated with 0.5 μM and 1.0 μM of compounds (**QCe**, **QAe**, **QPe**, **DMQAc**, **DMQPc**, **DMQAd**, **DMQPd**) or 0.1% DMSO as solvent control for 4 h. Afterwards, the intracellular Hoechst 33342 amount was detected by spectrofluorimetry (360 nm excitation/465 nm emission wavelengths, Tecan Infinite F200 Pro, Crailsheim, Germany). The relative fluorescence units (RFU) were correlated to the protein amount quantified by bicinchoninic acid assay (BCA; Thermo Scientific, Rockford, USA) following the manufacturer's instructions.

Determination of autofluorescence: The autofluorescence of compounds (**QCe**, **QAe**, **QPe**, **DMQAc**, **DMQPc**, **DMQAd**, **DMQPd**) was assessed by a modified Hoechst 33342 accumulation assay as described by Stockmann et al..[14] After cell seeding and cell incubation with these compounds, the intracellular fluorescence was measured by spectrofluorometer (360 nm excitation/465 nm emission wavelengths, Tecan Infinite F200 Pro, Crailsheim, Germany). Total intracellular fluorescence was corrected by subtracting the background and correlated to the protein amount quantified by BCA (Thermo Scientific, Rockford, USA) following manufacturing instructions.

Reversal of multidrug resistance: MDCKII cells were seeded as described in the WST-1 assay section, and treated with increasing concentrations of mitoxantrone (MXN) (0.01 μM up to 50 μM) or solvent (0.1% DMSO) for 48 h.[14] In order to detect a reversal of the ABCG2-mediated chemoresistance, compounds (**QCe**, **QAe**, **QPe**, **DMQAc**, **DMQPc**, **DMQAd**, **DMQPd**) were added to MXN in 1.0 μM for 48 h. The known ABCG2 inhibitor Ko143 (1.0 μM) was added as positive control. Afterwards, the WST-1 assay was performed as described above. The left-shift factor was calculated from IC_{50} minus SEM (standard error of mean) from the MXN-treated cells by IC_{50} plus SEM obtained from combined treatment of MXN and investigated compounds.

Cultivation of HT29 cells: Human colorectal adenocarcinoma HT29 cell line was acquired from American Type Culture Collection (ATCC, Rockville, USA) and was cultivated in HEPES (4-(2-hydroxyethyl)-1-piperazineethanesulfonic acid)-buffered RPMI-1640 medium supplemented with 2 mM L-glutamine and 0.01% sodium pyruvate (Capricorn Scientific GmbH, Hessen, Germany). Cell medium was additionally supplemented with 10% heat-inactivated fetal bovine serum (Capricorn Scientific GmbH, Hessen, Germany) and antibiotics (100 U/mL penicillin and 100 μg/mL streptomycin) (Biological Industries, Cromwell, USA). Cells were grown at 37 °C in a humidified atmosphere with 5% CO_2. Prior to cell passaging and seeding, cells were washed with phosphate-buffered saline (PBS; Sigma-Aldrich, St. Louis, USA) and detached by using 0.05% trypsin/0.02% EDTA (Capricorn Scientific GmbH, Hessen, Germany).

Reversal of MXN resistance in HT29 cells: HT29 cells were seeded in 96-well plates (Sarstedt, Nümbrecht, Germany) in a density of 6×10^3 cells/well, overnight. Cells were treated with increasing concentrations of MXN (0.01 μM up to 50 μM) alone or in combination with 1 μM of investigational compounds for 48 h. Solvent control (0.1% DMSO) and Ko143 (1 μM) were added as negative and positive controls, respectively. Afterwards, cell viability was assessed by MTT (3-(4,5-dimethylthiazol-2-yl)-2,5-diphenyltetrazolium bromide) assay (AppliChem, St. Louis, USA). In brief, the supernatant was discarded from wells and cells were incubated with MTT solution (0.5 mg/mL) for approximately half an hour until purple formazan crystals were formed. The crystals were dissolved in DMSO and the absorbance was measured with an automated microplate reader (LKB 5060–006; LKB Instruments, Vienna, Austria) at 540/670 nm wavelength. Data were expressed as a percentage of the negative control value obtained from cell cultures treated with a solvent, which was arbitrarily set to 100%. All experiments were repeated three times. The left-shift factor was calculated from IC_{50} minus SEM from the MXN-treated HT29 cells by IC_{50} plus SEM obtained from combined treatment of MXN and compounds (**QCe**, **QAe**, **QPe**, **DMQAc**, **DMQPc**, **DMQAd**, **DMQPd**).

Statistics: Data from WST-1 assays (N = 3) and Hoechst 33342 accumulation assay (N = 5) were tested for normality with Shapiro-Wilk test and subsequently analyzed by one-way ANOVA with Holm-Šidák post hoc test using SigmaPlot 14.5 (Systec Software, San Jose, CA, USA). IC_{50} values were defined as 50% reduced cell viability and calculated with SigmaPlot 14.5 by nonlinear regression.

In order to detect significant differences between groups treated with MXN, two-way ANOVA with Holm- Šidák post hoc test was performed by using SigmaPlot 14.5. With the exception of the autofluorescence data, all obtained values were normalized against vehicle control (0.1% DMSO) which was set as 1 and were expressed as mean ± SEM, calculated from at least three or five independent experiments for WST-1 or Hoechst 33342 accumulation assay, respectively.

Molecular docking/Computational methods: Docking studies were performed according to a recently published method.[14] Molecular structures were built with Avogadro 1.1.1,[31] geometries were optimized with ORCA 4.2.1, and electrostatic potential derived CHELPG charges were obtained from the ORCA-internal orca_chelpg program.[32] Cryo-electron microscopy (EM) structures of the human ABCG2 protein (PDB code 5NJ3)[27] and the co-crystallized MXN-ABCG2 substrate-protein structure (PDB code 6VXI)[29] were obtained from the Protein Data Bank (PDB; http://www.rcsb.org).[33] Molecular docking was performed with AutoDock 4.2.6 after previous protocols.[34,35] The AutoDock free energy scoring function had a standard error of 2–3 kcal/mol.[34] The UCSF ChimeraX software was used to visualize and render all molecular docking figures.[36]

Acknowledgements

We thank Cathleen Lakoma and Birte K. Scholz for skillful technical assistance and Wencke Leinung for meticulous synthetic support. This research was funded by the Ministry of Science, Technological Development and Innovation of the Republic of Serbia (grant number No. 451-03-47/2023-01/200007). Financial support from the Graduate School Leipzig School of Natural Sciences – Building with Molecules and Nano-objects (BuildMoNa) is gratefully acknowledged. Open Access funding enabled and organized by Projekt DEAL.

Conflict of Interests

The authors declare no conflict of interest.

Data Availability Statement

The data that support the findings of this study are available in the supplementary material of this article.

Keywords: breast cancer resistance protein · ABCG2 · carborane · multidrug resistance · cancer

[1] a) Y. H. Choi, A.-M. Yu, *Curr. Pharm. Des.* **2014**, *20*, 793–807; b) S. Wilkens, *F1000Prime Rep.* **2015**, *7*, 14.
[2] M. Dean, A. Rzhetsky, R. Allikmets, *Genome Res.* **2001**, *11*, 1156–1166.
[3] a) K. Moitra, M. Dean, *Biol. Chem.* **2011**, *392*, 29–37; b) V. Vasiliou, K. Vasiliou, D. W. Nebert, *Hum. Genomics.* **2009**, *3*, 281–290; c) A. Alam, K. P. Locher, *Annu. Rev. Biophys.* **2023**, *52*, 275–300.
[4] a) R. W. Robey, K. K. K. To, O. Polgar, M. Dohse, P. Fetsch, M. Dean, S. E. Bates, *Adv. Drug Delivery Rev.* **2009**, *61*, 3–13; b) S. Kukal, D. Guin, C. Rawat, S. Bora, M. K. Mishra, P. Sharma, P. R. Paul, N. Kanojia, G. K. Grewal, S. Kukreti, L. Saso, R. Kukreti, *Cell. Mol. Life Sci.* **2021**, *78*, 6887–6939; c) J. E. Diestra, G. L. Scheffer, I. Català, M. Maliepaard, J. H. M. Schellens, R. J. Scheper, J. R. Germà-Lluch, M. A. Izquierdo, *J. Pathol.* **2002**, *198*, 213–219; d) D. B. Iversen, N. E. Andersen, A.-C. Dalgård Dunvald, A. Pottegård, T. B. Stage, *Basic Clin. Pharmacol. Toxicol.* **2022**, *131*, 311–324.
[5] a) M. M. Gottesman, T. Fojo, S. E. Bates, *Nature reviews. Cancer* **2002**, *2*, 48–58; b) J.-P. Gillet, M. M. Gottesman, *Curr. Pharm. Biotechnol.* **2011**, *12*, 686–692.
[6] A. E. Stacy, P. J. Jansson, R. Des Richardson, *Mol. Pharmacol.* **2013**, *84*, 655–669.
[7] A. Tamaki, C. Ierano, G. Szakacs, R. W. Robey, S. E. Bates, *Essays Biochem.* **2011**, *50*, 209–232.
[8] R. W. Robey, P. R. Massey, L. Amiri-Kordestani, S. E. Bates, *Anti-Cancer Agents Med. Chem.* **2010**, *10*, 625–633.
[9] a) W. Mo, J.-T. Zhang, *Int. J. Biochem. Mol. Biol.* **2012**, *3*, 1–27; b) R. W. Robey, O. Polgar, J. Deeken, K. W. To, S. E. Bates, *Cancer Metastasis Rev.* **2007**, *26*, 39–57; c) Q. Mao, J. D. Unadkat, *AAPS J.* **2015**, *17*, 65–82; d) R. W. Robey, K. M. Pluchino, M. D. Hall, A. T. Fojo, S. E. Bates, M. M. Gottesman, *Nat. Rev. Cancer* **2018**, *18*, 452–464.
[10] P. Stockmann, M. Gozzi, R. Kuhnert, M.-B. Sárosi, E. Hey-Hawkins, *Chem. Soc. Rev.* **2019**, *48*, 3497–3512.
[11] Y. Chen, F. Du, L. Tang, J. Xu, Y. Zhao, X. Wu, M. Li, J. Shen, Q. Wen, C. H. Cho, Z. Xiao, *Mol. Ther. Oncolytics* **2022**, *24*, 400–416.
[12] a) F. Ali, N. S Hosmane, Y. Zhu, *Molecules* **2020**, *25*; b) S. Kulkarni, D. Bhandary, Y. Singh, V. Monga, S. Thareja, *Pharm. Ther.* **2023**, *251*, 108548.
[13] A. Marfavi, P. Kavianpour, L. M. Rendina, *Nat. Chem. Rev.* **2022**, *6*, 486–504.
[14] P. Stockmann, L. Kuhnert, W. Leinung, C. Lakoma, B. Scholz, S. Paskas, S. Mijatović, D. Maksimović-Ivanić, W. Honscha, E. Hey-Hawkins, *Pharmaceuticals* **2023**, *15*, 241.
[15] J. E. van Muijlwijk-Koezen, H. Timmerman, H. van der Goot, W. M. Menge, J. Frijtag Von Drabbe Künzel, M. de Groote, A. P. IJzerman, *J. Med. Chem.* **2000**, *43*, 2227–2238.
[16] R. A. Kasar, G. M. Knudsen, S. B. Kahl, *Inorg. Chem.* **1999**, *38*, 2936–2940.
[17] M. S. Scholz, L. M. Wingen, *Inorg. Chem.* **2017**, *56*, 5510–5513.
[18] a) P. Jansook, N. Ogawa, T. Loftsson, *Int. J. Pharm.* **2018**, *535*, 272–284; b) J. Rak, B. Dejlová, H. Lampová, R. Kaplánek, P. Matějíček, P. Cígler, V. Král, *Mol. Pharm.* **2013**, *10*, 1751–1759; c) J. Rak, R. Kaplánek, V. Král, *Bioorg. Med. Chem. Lett.* **2010**, *20*, 1045–1048; d) K. Uekama, F. Hirayama, T. Irie, *Chem. Rev.* **1998**, *98*, 2045–2076.
[19] M. K. Krapf, J. Gallus, V. Namasivayam, M. Wiese, *J. Med. Chem.* **2018**, *61*, 7952–7976.
[20] L. Kuhnert, R. Kuhnert, M. B. Sárosi, C. Lakoma, B. K. Scholz, P. Lönnecke, E. Hey-Hawkins, W. Honscha, B. K. Scholz, *Mol. Onc.* **2023**, in print, https://doi.org/10.1002/1878-0261.13527.
[21] R. Feldman, B. L. Abbott, S. K. Reddy, M. Castro, *J. Clin. Oncol.* **2015**, *33*, 11108.
[22] a) C. Tian, C. B. Ambrosone, K. M. Darcy, T. C. Krivak, D. K. Armstrong, M. A. Bookman, W. Davis, H. Zhao, K. Moysich, H. Gallion, J. A. DeLoia, *Gynecol. Oncol.* **2012**, *124*, 575–581; b) C.-P. Wu, C.-H. Hsieh, Y.-S. Wu, *Mol. Pharm.* **2011**, *8*, 1996–2011; c) K. Yoh, G. Ishii, T. Yokose, Y. Minegishi, K. Tsuta, K. Goto, Y. Nishiwaki, T. Kodama, M. Suga, A. Ochiai, *Clin. Cancer Res.* **2004**, *10*, 1691–1697; d) R. W. Robey, Y. Honjo, K. Morisaki, T. A. Nadjem, S. Runge, M. Risbood, M. S. Poruchynsky, S. E. Bates, *Br. J. Cancer* **2003**, *89*, 1971–1978.
[23] a) D. D. Ross, W. Yang, L. V. Abruzzo, W. S. Dalton, E. Schneider, H. Lage, M. Dietel, L. Greenberger, S. P. Cole, L. A. Doyle, *J. Natl. Cancer Inst.* **1999**, *91*, 429–433; b) M. Nakagawa, E. Schneider, K. H. Dixon, J. Horton, K. Kelley, C. Morrow, K. H. Cowan, *Cancer Res.* **1992**, *52*, 6175–6181.
[24] D. Martínez-Maqueda, B. Miralles, I. Recio, in *The Impact of Food Bioactives on Health: in vitro and ex vivo models. HT29 Cell Line*, (Eds.: K. Verhoeckx, P. Cotter, I. López-Expósito, C. Kleiveland, T. L. A. Mackie, T. Requena, D. Swiatecka, H. Wichers) Springer, Cham (CH), 2015, pp. 113–124.
[25] a) M. Kühnle, M. Egger, C. Müller, A. Mahringer, G. Bernhardt, G. Fricker, B. König, A. Buschauer, *J. Med. Chem.* **2009**, *52*, 1190–1197; b) E. J. Wang, C. N. Casciano, R. P. Clement, W. W. Johnson, *Arch. Biochem. Biophys.* **2000**, *383*, 91–98.
[26] B. Dudas, X. Decleves, S. Cisternino, D. Perahia, M. A. Miteva, *Comput. Struct. Biotechnol. J.* **2022**, *20*, 4195–4205.
[27] N. M. I. Taylor, I. Manolaridis, S. M. Jackson, J. Kowal, H. Stahlberg, K. P. Locher, *Nature* **2017**, *546*, 504–509.
[28] S. M. Jackson, I. Manolaridis, J. Kowal, M. Zechner, N. M. I. Taylor, M. Bause, S. Bauer, R. Bartholomaeus, G. Bernhardt, B. Koenig, A. Buschauer,

H. Stahlberg, K.-H. Altmann, K. P. Locher, *Nat. Struct. Mol. Biol.* **2018**, *25*, 333–340.
[29] B. J. Orlando, M. Liao, *Nat. Commun.* **2020**, *11*, 2264.
[30] R. K. Harris, E. D. Becker, S. M. Cabral De Menezes, R. Goodfellow, P. Granger, *Solid State Nucl. Magn. Reson.* **2002**, *22*, 458–483.
[31] M. D. Hanwell, D. E. Curtis, D. C. Lonie, T. Vandermeersch, E. Zurek, G. R. Hutchison, *J. Cheminf.* **2012**, *4*, 17.
[32] F. Neese, *WIREs Comput. Mol. Sci.* **2018**, *8*.
[33] H. M. Berman, J. Westbrook, Z. Feng, G. Gilliland, T. N. Bhat, H. Weissig, I. N. Shindyalov, P. E. Bourne, *Nucleic Acids Res.* **2000**, *28*, 235–242.
[34] G. M. Morris, R. Huey, W. Lindstrom, M. F. Sanner, R. K. Belew, D. S. Goodsell, A. J. Olson, *J. Comput. Chem.* **2009**, *30*, 2785–2791.
[35] R. Kuhnert, M.-B. Sárosi, S. George, P. Lönnecke, B. Hofmann, D. Steinhilber, S. Steinmann, R. Schneider-Stock, B. Murganić, S. Mijatović, D. Maksimović-Ivanić, E. Hey-Hawkins, *ChemMedChem* **2019**, *14*, 255–261.
[36] E. F. Pettersen, T. D. Goddard, C. C. Huang, G. S. Couch, D. M. Greenblatt, E. C. Meng, T. E. Ferrin, *J. Comput. Chem.* **2004**, *25*, 1605–1612.

Manuscript received: September 19, 2023
Revised manuscript received: November 27, 2023
Accepted manuscript online: November 27, 2023
Version of record online: ■■, ■■

RESEARCH ARTICLE

Carborane comes first! Overcoming multidrug resistance mediated by ABCG2 efflux transporter is a major challenge in cancer therapy. The previously reported carborane-based compound **DMQCd** shows advantages compared with the corresponding adamantyl and phenyl analogues in terms of cytotoxicity, inhibition of the human ABCG2 transporter and the ability to reverse ABCG2-mediated mitoxantrone resistance.

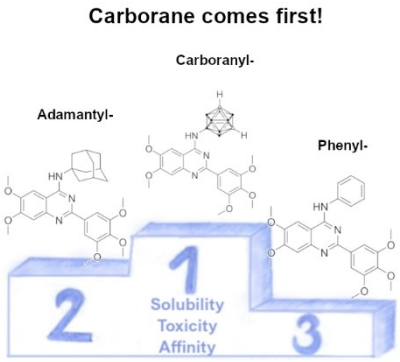

Dr. P. Stockmann, Dr. L. Kuhnert, Dr. T. Krajnović, Prof. S. Mijatović, Prof. D. Maksimović-Ivanić, Prof. W. Honscha, Prof. E. Hey-Hawkins**